

UNCLASSIFIED

AD 273 604

*Reproduced
by the*

**ARMED SERVICES TECHNICAL INFORMATION AGENCY
ARLINGTON HALL STATION
ARLINGTON 12, VIRGINIA**



UNCLASSIFIED

NOTICE: When government or other drawings, specifications or other data are used for any purpose other than in connection with a definitely related government procurement operation, the U. S. Government thereby incurs no responsibility, nor any obligation whatsoever; and the fact that the Government may have formulated, furnished, or in any way supplied the said drawings, specifications, or other data is not to be regarded by implication or otherwise as in any manner licensing the holder or any other person or corporation, or conveying any rights or permission to manufacture, use or sell any patented invention that may in any way be related thereto.

CATALOGED BY ASTIA
AS AD NO. 273604

273 604

ASD TECHNICAL REPORT 61-595

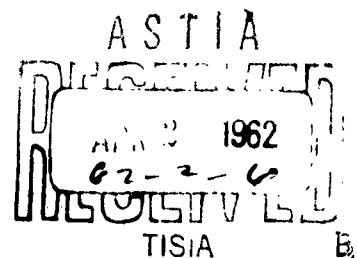
IMPACT STUDIES ON LUNAR DUST MODELS AT VARIOUS VACUUMS

RICHARD LANSING GEER, B. E.

1ST LT., USAF

TECHNICAL REPORT No. ASD TR 61-595

JANUARY 1962



AERONAUTICAL SYSTEMS DIVISION
AIR FORCE SYSTEMS COMMAND
UNITED STATES AIR FORCE
WRIGHT-PATTERSON AIR FORCE BASE, OHIO

PROJECT No. 8119, TASK No. 811918

NOTICES

When Government drawings, specifications, or other data are used for any purpose other than in connection with a definitely related Government procurement operation, the United States Government thereby incurs no responsibility nor any obligation whatsoever; and the fact that the Government may have formulated, furnished, or in any way supplied the said drawings, specifications, or other data, is not to be regarded by implication or otherwise as in any manner licensing the holder or any other person or corporation, or conveying any rights or permission to manufacture, use, or sell any patented invention that may in any way be related thereto.

Qualified requesters may obtain copies of this report from the Armed Services Technical Information Agency, (ASTIA), Arlington Hall Station, Arlington 12, Virginia.

This report has been released to the Office of Technical Services, U. S. Department of Commerce, Washington 25, D. C., for sale to the general public.

Copies of ASD Technical Reports and Technical Notes should not be returned to the Aeronautical Systems Division unless return is required by security considerations, contractual obligations, or notice on a specific document.

PREFACE

This study is the result of a request by the Logistics, Maintenance and Support Techniques Section of the Flight Accessories Laboratory of ASD for an investigation of lunar environmental simulation. Because of the time limitations, I could study in detail only one aspect of lunar simulation, that of the relationship between the lunar dust model and the degree of vacuum in the simulator. Some other aspects of lunar simulation that were investigated in less detail are covered in appendixes to this report.

I had basically two choices in carrying out the main work reported here, the impact studies on lunar dust models: I could study in great detail one model at one or two levels of vacuum to establish, beyond doubt, all its characteristics under the given test conditions; or I could study a broad range of models at many levels of vacuum with just enough controls to insure the general validity of my results as an over-all picture of lunar dust behavior. The former approach had been used in two or three previous studies (see Chapter II) and had yielded little useful information. I chose the latter approach, with its attendant hazard of leaving many relatively small points unsettled.

This report is not meant to be definitive of lunar-dust model behavior in a vacuum. I hope, rather, that it will be preliminary to other reports concerning more detailed studies of the dynamic behavior of these dusts and will resolve the uncertainties in my work.

As will shortly be apparent to any geologist reading this report, I am not a geologist. Neither am I knowledgeable in soil mechanics. Since I am qualified for this investigation only by my keen interest in the subject, it is very probable that some errors of fact have crept into the report. I can only hope they are not too significant.

It is impossible to list and thank here all those who were kind enough to answer my correspondence. Special thanks are due to Dr. Jack Green of Aero-Space Laboratories, North American Aviation, Inc., for his courtesy when I visited him in Downey, California. His guidance has been very useful. Dr. Springer of the University of Dayton is to be thanked for his suggestions of sources of dust specimens. Dr. John Stephens of The Ohio State University and Mr. Donald Richter of the Hawaiian Volcano Observatory deserve thanks for their generosity in supplying specimens. I would also like to thank my parents for assembling and sending me specimens from the southwestern desert areas. My thanks to my sponsors, Mr. Hildebrandt, Mr. Tackis, and Mr. Washburn for their welcome and timely administrative assistance; to the men of the Space and Atmospheric Deterioration Branch of the Environmental Division, ASD (particularly to Mr. Sam Kesling) for their patient, good-humored support of this project; and to the Flight Control Laboratory, ASD, for putting up with my clutter in their work area. Finally I must thank my wife for doing much more typing than complaining about my rough drafts, and for services far beyond the call of duty in pulverizing my rock specimens.

This thesis was presented to the faculty of the School of Engineering of the Institute of Technology, Air University, in partial fulfillment of the requirements for the Degree of Master of Science. Only minor editing has been done on this paper to make it conform with the requirements for an Aeronautical Systems Division Technical Report.

VITA

Richard Lansing Geer was born on 29 September 1933 in Portland, Oregon, the son of Dr. Charles Willard Geer and Mary Wells Geer. After graduation in 1950 from Long Beach Polytechnic High School, Long Beach, California, he attended Long Beach City College, and Willamette University, Salem, Oregon, taking a liberal arts curriculum. In 1953, he entered the University of Southern California, and graduated in June 1955 with a degree of Bachelor of Engineering with a major in mechanical engineering (aero-option). He received his reserve commission as a second lieutenant at that time. After working for Boeing Airplane Company and attending the University of Washington for a brief period, he was called to active duty in November 1955. His military assignments prior to his coming to the Institute of Technology have been confined to the Aero-Medical Laboratory of Wright Air Development Center, where he worked on manned balloon gondola design and test, escape system studies, and space cabin design.

ABSTRACT

An analysis of the factors relevant to lunar environmental simulation show that the dynamic behavior of lunar dust models in various vacuums must be studied to establish the degree of vacuum required of a lunar simulator. Various silicic and basaltic rock dusts were selected as lunar dust models and tested under a range of vacuums. Although crater width measurements indicate lunar dust models do not change their resistance to impact at vacuums beyond 1×10^{-5} mm Hg, depth of penetration measurements do show a continuous change in resistance up to 1×10^{-5} mm Hg, the limit of the test. The behavior of lunar dust particles depended upon both particle size distribution and particle microstructure. The effects of hold times at vacuum, container walls, dust shallowness, and the composition of the residual atmosphere on dust behavior are analyzed. Recommendations are made for follow-up studies.

TABLE OF CONTENTS

Section		Page
1	Introduction	1
	The Problem of Lunar Environmental Simulation	1
	The Plan of This Report	3
	A Preliminary Summary of Conclusions	3
2	The Dusts Studied	4
	Origin of the Dusts	4
	Particle Size Distribution of the Dusts	6
	Microstructure of the Dusts	9
3	The Test Procedure	16
	The Time History of the Data Runs	16
	The Vacuum Equipment	19
	Methods of Measuring the Effects of Impact	19
	The Calibration and Check Runs	20
4	Discussion of the Test Results	31
	Variation of Impact Parameter with Degree of Vacuum	31
	Comparison of the Behavior of the Various Dusts	45
	Possible Explanations of Variations in Impact Behavior at Vacuum	47
	Meaning of the Results for Lunar Environmental Simulation	48
5	Conclusions	49
	Summary	49
	Recommendations	49
Appendix		
A	A Survey of Lunar Surface Conditions	51
B	Reduced Gravity Simulation in a Lunar Environmental Simulator	55
C	A Partial Survey of Present Space Simulator Facilities Relevant to the Design of a Lunar Environmental Simulator	58
D	The Limit of Convection with Decreasing Pressure	60
E	High-Vacuum Friction	63
F	High-Vacuum Exposure of Lunar Rock Models	64
G	A Glossary of Astronomical and Geological Terms	66
List of References		68

LIST OF ILLUSTRATIONS

Figure		Page
1	Comparative Particle Size Distribution	9
2	Natural Silicic Dusts of Volcanic Origin; 3-F Pumice and Death Valley Silicic	11
3	Natural Silicic Dust of Volcanic Origin from Mt. Katmai	12
4	Magnetic Volcanic Dusts	13
5	Pulverized Dusts of Volcanic Origin	14
6	Pulverized Hawaiian Basaltic Dusts	15
7a	Schematic Diagram of the Apparatus	17
7b	Layout of the Apparatus	18
7c	Operation of the Electromagnet	18
8	Effect of Hold Time on Depth of Penetration and Crater Rim Diameter for Death Valley Silicic Dust at 1×10^{-2} and 5×10^{-5} mm Hg	21
9	Variation of Crater Parameters with Distance from Cannister Wall	22
10	Effect of Dust Shallowness (Linear Extrapolation)	24
11	Depth of Penetration, Death Valley Silicic Dust, 2.2 Inches Deep	25
12	Crater Rim Diameter, Death Valley Silicic Dust, 2.2 Inches Deep	25
13	Comparison of Depth of Penetration in Air-Helium Atmosphere with Carbon Dioxide-Hydrogen Atmosphere	27
14	Comparison of Crater Rim Diameter in Air-Helium Atmosphere with Carbon Dioxide-Hydrogen Atmosphere	28
15	Ball Drop Pattern and Effect of Local Density Irregularities	30
16	Cratering Effects of Death Valley Silicic Dust at Various Pressures with a Depth of 2.2 Inches	32
17	Cratering Effects of Hawaiian Phreatomagmatic Basaltic Dust at Various Pressures with a Depth of 2.2 Inches	33

LIST OF ILLUSTRATIONS (CONT'D)

Figure		Page
18	Cratering Effects of 3-F Pumice Dust at Various Pressures	34
19a and b	Cratering Effects of Mt. Katmai Silicic Dust at Various Pressures with a Depth of 2.2 Inches	35-36
20	Cratering Effects of Ground Silicic Acidic Tuff Dust at Various Pressures with a Depth of 1 Inch	37
21	Depth of Penetration in Dusts 2.2 Inches Deep	39
22	Depth of Penetration in Dusts 1.3 Inches Deep	40
23	Depth of Penetration in Dusts 1.0 Inch Deep	40
24	Crater Rim Diameter in Dust 2.2 Inches Deep	41
25	Crater Rim Diameter in Dust 1.3 Inches Deep	41
26	Crater Rim Diameter in Dust 1.0 Inch Deep	42
27	Maximum Diameter of Cratering in Hawaiian Phreatomagmatic Dust 2.2 Inches Deep	42
28	Maximum Diameter of Cratering in Ground Silicic Tuff Dust 1.0 Inch Deep	43
29	Decrease in Free-Air Convection with Increasing Altitude	62
30	Volcanic Rock Specimens After Exposure to Vacuum	65

LIST OF TABLES

Table		Page
1	Dust Particle Size Distribution	7
2	Particle Size Distribution of Dusts Used by Other Researchers	8
3	Estimated Data Scatter	29
4	Comparison of Parameters at Various Pressures	45
5	Dust Comparison Summary	46
6	Analysis of Gases from Kilauea Volcano, 1917-1919	54
7	Increase of Mean Free Path with Decrease in Pressure	61

SECTION 1

INTRODUCTION

THE PROBLEM OF LUNAR ENVIRONMENTAL SIMULATION

The testing of systems and subsystems in a laboratory environment simulating, as closely as possible, the intended operational environment is an accepted part of the development process for new equipment. Nowhere is this simulation and testing more important than in the development of equipment designed to operate on the moon. There are, however, no lunar environmental simulators in existence, and there are no firm plans to build any. The uncertainty inherent in such a design has forestalled any attempt to weigh the various factors to be simulated, the relative importance of each, the relative uncertainty inherent in each, and the effectiveness with which each can be simulated.

Five factors must be considered in simulating a lunar environment: reduced gravity, exposure to particulate radiation, extremes of thermal radiation, surface structure, and degree of vacuum on the surface. (See Appendix A for a discussion of these factors.)

Reduced gravity is the factor which both can and cannot be most easily simulated. As an example, for a traction test of a "moon-tank" in a lunar environmental simulator, it would be simple to reduce the weight on the treads to one-sixth ambient (by removing most of the equipment not connected with the driving mechanism) and to thus achieve an effective traction test, but this would be simulating reduced gravity by model rather than by simulator. No test simulator can reduce gravity, but certain gravitational effects may be simulated by models. (See Appendix B for details of reduced gravity simulation by model.) Thus the reduced gravity of the moon does not impose a direct requirement on the lunar simulator.

The amount of particulate radiation that reaches the lunar surface is still a matter of some conjecture. Although certain types of equipment designed for lunar use should be tested in an approximation of the lunar particulate radiation environment, apparently there is little reason to make this test simultaneously with the mechanical and thermal tests to be provided by the lunar simulator. The particulate radiation environment, for all practical purposes, will have effects independent of the mechanical and thermal environment. Thus, the effects of such radiation as solar electrons and primary cosmic ray particles may (and for simplicity, should) be considered apart from the requirements of a lunar environmental simulator.

The extremes of electromagnetic and, more specifically, thermal radiation encountered on the moon present a definite requirement for the lunar simulator. Fortunately, however, this factor has been simulated in many space simulation chambers (to a greater or lesser degree of verisimilitude) and techniques that may be used successfully for lunar environmental chambers are well established. (See Appendix C for a description of these techniques.) Simulating the thermal radiation environment is primarily a design problem, and it will not be considered further in this report.

The two remaining factors, the surface structure and the degree of vacuum on the moon, are the chief unknowns and are the most important factors governing the design of a simulator. These two factors are interrelated.

The surface composition of the moon may not be simulated with any certainty -- at least not until lunar rockets can return with large samples of the lunar surface. However, a technique is available which will obtain usable, albeit not guaranteed, results. It is generally agreed that lunar rock and dust consist of only a few main types (Refs. 16:11, 31:1667-1680, 32:19, 14:164). These types are also found on earth in many specific forms (Ref. 16:11). Therefore, if a sufficiently broad selection is made from these "moon-possible" terrestrial rocks and dust, it may be argued that somewhere in the selection are dusts and rock that very closely approximate actual lunar material. This is the procedure that has been followed in this study.

The degree of vacuum on the moon has been estimated at from 0.076 mm Hg (Ref. 15:130) to 1.52×10^{-10} mm Hg (or the vacuum of interplanetary space - 10^3 particles per cubic centimeter) (Refs. 6:1606, 12:1040-6). However, it would be impossible to make lunar simulation runs at selected vacuums between 0.0001 atmospheres and the vacuum of interplanetary space, knowing that the true lunar environment was somewhere in between. The best vacuum obtainable today for a chamber in the size range of a lunar simulator is 10^{-7} mm Hg (Ref. 5:9). (See also Appendix C.) Past 10^{-9} mm Hg or so, increasing the degree of vacuum is first prohibitively expensive, and then highly impractical.

The question to be asked, then, is not "What vacuum must we obtain to duplicate the vacuum of the moon?" but rather, "What vacuum must we obtain to duplicate all the effects of a high lunar vacuum on the systems under test?"

The presence of a high vacuum of unknown quantity on the moon will make itself manifest in three ways that must be duplicated by the vacuum of a lunar simulator. The first is that there must be no convective heat transfer within the simulator. This is easily obtained at vacuums of about 10^{-3} mm Hg (see Appendix D). The second is that the phenomenon of vacuum friction must be present; that is, the coefficient of friction should increase sharply due to the presence of a high vacuum. This phenomenon, which is of considerable importance in the operation of equipment in high vacuum, occurs at 10^{-6} mm Hg (Ref. 30:104-107 and also Appendix E) or lower vacuums. The third is in the effect that that vacuum has on the dust covering the lunar surface. (For a more detailed discussion of lunar surface dust, see Appendix A)

Dust under vacuum has sharply different load-bearing characteristics than dust in an atmosphere. The investigation of the dynamic response to impact at various degrees of vacuum on various samples of terrestrial dust representative of types considered likely to be on the moon will determine a limit (or lack of a limit) beyond which no further increase in vacuum changes the dynamic behavior of the dust. This limit, or lack thereof, may then be compared with the other limits mentioned and a realistic requirement may be established for the vacuum necessary for lunar environmental simulation. For example, if the lunar dust models do not change their behavior below 10^{-4} mm Hg pressure, it will be possible to obtain effective lunar simulation in a chamber operating between 10^{-4} mm Hg and that pressure at which the coefficient of friction no longer increases with increasing vacuum. If the lunar dust models continue to change their behavior past the limit of vacuum available for this study (10^{-5} mm Hg), any lunar environmental simulator must provide a vacuum greater than that, and studies must be pursued at still higher vacuums to establish the terminal point of the phenomena.

THE PLAN OF THIS REPORT

This report first tells how various types of rock dusts were selected as lunar dust models and how samples of these dusts were obtained for testing. It then shows how these dusts were classified by particle size distribution and microstructure.

The manner in which impact studies were made of these dusts is then discussed. The experimental techniques, equipment, and measurements are shown. The sources of error and the necessary calibration and correction factors are analyzed.

Next, the test results are discussed to show how the various impact parameters change with degree of vacuum for each of the dusts studied. The effect of particle size distribution and microstructure is shown and some possible explanations are discussed. The meaning of the results for lunar environmental simulation is explored.

Finally, conclusions are drawn from the test results and the need for additional testing is established.

In Appendix A may be found a survey of lunar surface conditions which should be useful as background information. Appendixes B through F list important supplementary information of direct bearing on lunar environmental simulation, but of little or no direct application to impact studies on lunar dust models. Appendix G contains a glossary of astronomical and geological terms.

A PRELIMINARY SUMMARY OF CONCLUSIONS

It will be shown that not only particle size distribution, but also microstructure, must be considered in analyzing the behavior of a lunar dust model under vacuum. It will be shown that no single dust model can be adequate for design or test purposes. Finally, it will be shown that any valid experiment on the behavior of lunar dust models must consider and evaluate the effect of a large number of test variables.

SECTION 2

THE DUSTS STUDIED

The most important item in a study of lunar dust models is the accuracy of the models. As was mentioned in the introduction, these models must be representative of the probable lunar dusts, and as broadly representative as possible. The dusts used as models must cover a broad range of chemical composition, particle size distribution, and microstructure in order that one or more of them will approximate one or more actual lunar dusts in behavior.

ORIGIN OF THE DUSTS

As is discussed in more detail in Appendix A, there are two key sets of facts (or unanimous opinions) about the moon that determine the type of rocks and dust we may expect to find there. The first is that the lunar surface is composed chiefly of rock analogous to terrestrial silicic rock in the mountains and lighter colored areas (Ref. 15:34), and of rock analogous to terrestrial basaltic rock in the maria or darker colored areas (Ref. 15:42).^{*} The second is that the main selenological (lunar geological) process operating now or in the past, which accounts for its crater-scarred surface, is either meteoric or volcanic.

Thus, in selecting a working hypothesis concerning the lunar surface conditions on which to base our dust selection, two main choices present themselves: (1) The lunar dusts are produced mainly by very high-speed impact of stony and nickel-iron meteorites on silicic and basaltic rock surface. (2) The lunar dusts are produced principally by volcanic processes in basaltic and silicic rocks.

In considering which hypothesis to follow or whether, in fact, it is permissible to make a choice, three questions must be answered: (1) Upon which side is the weight of the evidence? (2) What effect does a wrong guess have upon the results? (3) Granted that a given hypothesis is correct, can it be translated into terms of lunar dust models?

In weighing the merits of the meteoric versus the volcanic hypothesis, one is struck by the violence of the opinion on either side. Most American selenologists prefer the meteoric theory, and many have written articles and books devoted exclusively to upholding this idea (Refs. 31 and 4, in toto). On the other hand, most English selenologists prefer the volcanic hypothesis. V. A. Firsoff (Ref. 15) and P. Moore (Ref. 22) devote whole chapters to this concept. It appears that the National Aeronautics and Space Administration leans toward the meteoric theory.^{**} However, in the author's opinion, a careful examination of all the evidence will lead to the acceptance of the volcanic origin for the lunar features.

^{*} See also Refs. 16, 31, and 14, which discuss this concept throughout each work. For definitions of the various geological terms used in this section of the thesis, such as "silicic," "basaltic," "dust," etc., see Appendix G.

^{**} Letter from Dr. L. D. Jaffe, Chief, Materials Research Section, Jet Propulsion Laboratory (NASA), Pasadena, California (23 May 1961).

If the moon's surface was, in fact, formed by the impact of giant meteorites, the surface would have been compacted and much coarse dust ("rock flour") would have been produced by the pulverization of both target area and missile. On the other hand, if the moon's surface was formed by volcanic processes, the underlying rock would be light and frothy in places and the dusts would tend to have the smaller particle sizes characteristic of volcanic dusts (see Fig. 1). Now, vehicles designed and tested to operate in an environment that includes rock froth and fine dust as well as lava beds should operate as well, or better, on densely-packed surfaces covered with coarse dust; but vehicles designed for dense-surface operation are not likely to function on soft surfaces. In other words, a "weasel" can go both where a "Jeep" can go and where it can't go, but the reverse is not true. Therefore, for conservative design, the volcanic hypothesis should be used.

If the meteoric hypothesis is used, the dusts will include varying amounts of iron-nickel particles, since the composition of a large proportion of meteorites is iron-nickel. Unfortunately, no one can estimate the proportion of iron-nickel meteorites in the supposed great in-fall on the moon eons ago. Neither is it possible to estimate in what form the iron-nickel manifests itself in the lunar dust (as particles, drops, fragments, or lumps). Therefore, it is impossible to build a dust model based specifically on the meteoric-impact theory without ignoring the major effect of adding iron-nickel particles to the dust. (See also Ref. 16:11.) The volcanic concept, however, lends itself readily to the construction of dust models. Both basaltic and silicic volcanic dusts occur naturally on earth in a wide variety of types.

For the above reasons, the volcanic concept of the origin of most of the selenological features was selected as the working hypothesis. At the same time, it was decided to test dusts created by artificially pulverizing basaltic and silicic rocks to maintain the greatest possible validity of results and to compare the behavior of dusts formed by two different processes.

Silicic dusts were obtained from two sources:

- (1) Tecopa, California (half way between Baker and Death Valley Junction, just east of Death Valley) and from the A. T. Wagner Company of Detroit, Michigan. This dust is a very fine pumice, designated 3-F, used for foundry work. No further information on its origin was obtainable.
- (2) From Mt. Katmai, also known as Katmai Volcano, in Alaska's Aleutian Range. (This dust was obtained on loan from The Ohio State University Department of Geology.)

Silicic rock was obtained from the southern California desert region in the form of a decomposed acidic tuff, and from Italy in the form of pumice (probably from the Naples area). This was ground to produce a coarse dust.

All basaltic specimens were obtained from the Hawaiian Volcano Observatory on Hilo, specifically, from Kilauea Volcano. A basaltic dust was obtained that had its origin in the 1790 phreatomagmatic eruption. Specimens of basaltic pumice and reticulite were pulverized to a coarse powder.

Although the dusts are of various ages and have been exposed to various types of weatherings, many of them are essentially unchanged from the as-produced state. The 2500-year-old reticulite and the two-year-old basaltic pumice showed identical microstructure. The Mt. Katmai dust was collected soon after the great 1912 eruption. Of course, some of the material has weathered in a manner foreign to a lunar environment.

In fact, it must be admitted that none of the material was produced under anything like lunar conditions. But, since it is not known how lunar and terrestrial volcano dusts would differ, and since there is no evidence to indicate that they do differ, we can only suppose that lunar volcanos and terrestrial volcanos produce about the same kind of dust.

Although the subject is covered in more detail in Appendix A, some final words on the origin of lunar dusts are appropriate here. Neither the meteoric nor the volcanic schools claim that the process they champion can account for all the dust. Dusts may be and probably are formed by thermal shock, corpuscular radiation, meteoric impact, volcanic, tectonic, and accretive processes (Ref. 2:3). However, the major process of dust formation must be either volcanic alone, meteoric and volcanic, or (least likely) meteoric alone.

PARTICLE SIZE DISTRIBUTION OF THE DUSTS

Previous and current studies of lunar dust models have often tended to classify dusts on the basis of particle size alone, neglecting the geological classification and microstructure. While particle size distribution is not the only parameter of interest in dust classification, it is certainly extremely important.

In order to establish the particle size distribution, the samples (or, in some cases, the total available amount of dust) were placed in an arrangement of successively finer sieves, which was then installed in a Combs Gyratory Sifting Machine. The machine was run for from 20 to 45 minutes, depending on the dust being sifted, until no more dust was observed to pass from any one sieve to the next below. The samples were then weighed and a particle size distribution by weight was calculated. Table 1 shows this distribution for the seven dusts tested and Table 2 shows the distribution for three dust types used by other researchers for lunar dust models. The dusts are listed approximately in order of decreasing coarseness. The dust specimens used by the other researchers are listed in Table 2, as different series of sieves were used in finding size distributions.

A few words about the other lunar-dust-model studies should be interjected here. First, the models listed in Table 2 are the only models that have been tested quantitatively, so far as is known.* Grumman** and Bendix*** have test programs initiated and Norair (Ref. 23) is continuing with their program and with dusts other than those listed in Table 2. North American (Ref. 2:23-38) made a study but did not quantify their data or their particle size distribution. This lack of comparability is due primarily to each researcher studying a different aspect of the problem and using different measurement techniques.

* A letter from Floyd L. Thompson, Director, Langley Research Center, Langley Field, Virginia (1 August 1961) indicates that NASA has studies in progress using aluminum oxide, plaster of paris, and flour as lunar dust models. Apparently the aluminum oxide is "600 to 40 grit", but no information was given on the other particles.

** Telephone conversation (1 May 1961) and letter (21 June 1961) from Messrs J. D. Halajian and R. Stewart, project engineers, Grumman Aircraft Engineering Corporation, Bethpage, New York.

*** Interview with Mr. R. Immonen, project engineer, Bendix Systems Division, Bendix Corporation, Ann Arbor, Michigan (23 June 1961).

The "NASA olivine basalt" is a dust used as a lunar soil model by the National Aeronautics and Space Administration (JPL) for their design and experimental work on lunar vehicles. This is an unweathered basalt from Pisgah Crater, San Bernardino County, California, crushed to the size distribution indicated in Table 2. Dr. Jaffe states that they may go on to tests using other rock types, but they have not started yet.*

TABLE 1
DUST PARTICLE SIZE DISTRIBUTION

Dust	Percent by Weight of Particles Larger Than							
	590 μ *	149 μ	105 μ	88 μ	74 μ	44 μ	38 μ	0 μ
Ground Hawaiian Basaltic	2.75	56.0	73.1	80.7	84.3	93.4	95.1	100
Ground Italian Pumice	1.97	50.6	61.0	66.8	70.2	79.6	81.9	100
Ground Silicic Tuff	0	39.3	48.1	53.4	56.6	68.4	71.1	100
Hawaiian Phreatomagmatic Basaltic	0.29	22.0	32.5	40.4	45.4	63.4	68.4	100
Mt. Katmai Silicic	0	18.7	27.0	31.5	34.2	44.4	57.9	100
Death Valley Silicic	0.66	6.94	15.7	25.8	29.8	50.1	55.8	100
3-F Pumice	0	0.82	2.9	5.86	7.73	19.6	23.7	100

*1 μ = 10⁻³ millimeters

* Letter from Dr. L. D. Jaffe, Chief, Materials Research Section, Jet Propulsion Laboratory (NASA), Pasadena, California (23 May 1961).

TABLE 2

PARTICLE SIZE DISTRIBUTION OF DUSTS USED BY OTHER RESEARCHERS

Dust	Percent, by Weight, of Particles Larger Than									
	417 μ	208 μ	147 μ	104 μ	74 μ	43 μ	31 μ	20 μ	3 μ	0 μ
NASA Olivine* Basalt	8	22	35	52	73	81	95	99	99.7	100
Norair Sand and Dust Mixture** (per MIL-E-5272A)			149 μ	105 μ	74 μ	44 μ				0 μ
			0	2	10	25				100
Univ. of Michigan Sea Sand***	420 μ	177 μ		90 μ		44 μ				
	0	0 100		0 100		100	(Grade 1) (Grade 2) (Grade 3)			

* (From a letter by Dr. L. D. Jaffe, Chief, Materials Research Section, Jet Propulsion Laboratory (NASA), Pasadena, California (23 May 1961.)

** From Ref. 23.

*** From Ref. 8:23-33.

The University of Michigan used sea sand as their lunar dust model (Ref. 8:24-33). A continuation of this work is in the planning stage.*

A graph of the data listed in Table 1 is presented in Figure 1. (The University of Michigan and Norair data are not plotted due to an insufficiency of data points.)

Although no lower limit is given to particle size, it is generally agreed that the smallest particles in natural volcanic dusts is 4 μ (Ref. 20:357).

* Letter from W. E. Fensler, research engineer, University of Michigan, Ann Arbor, Michigan (6 June 1961).

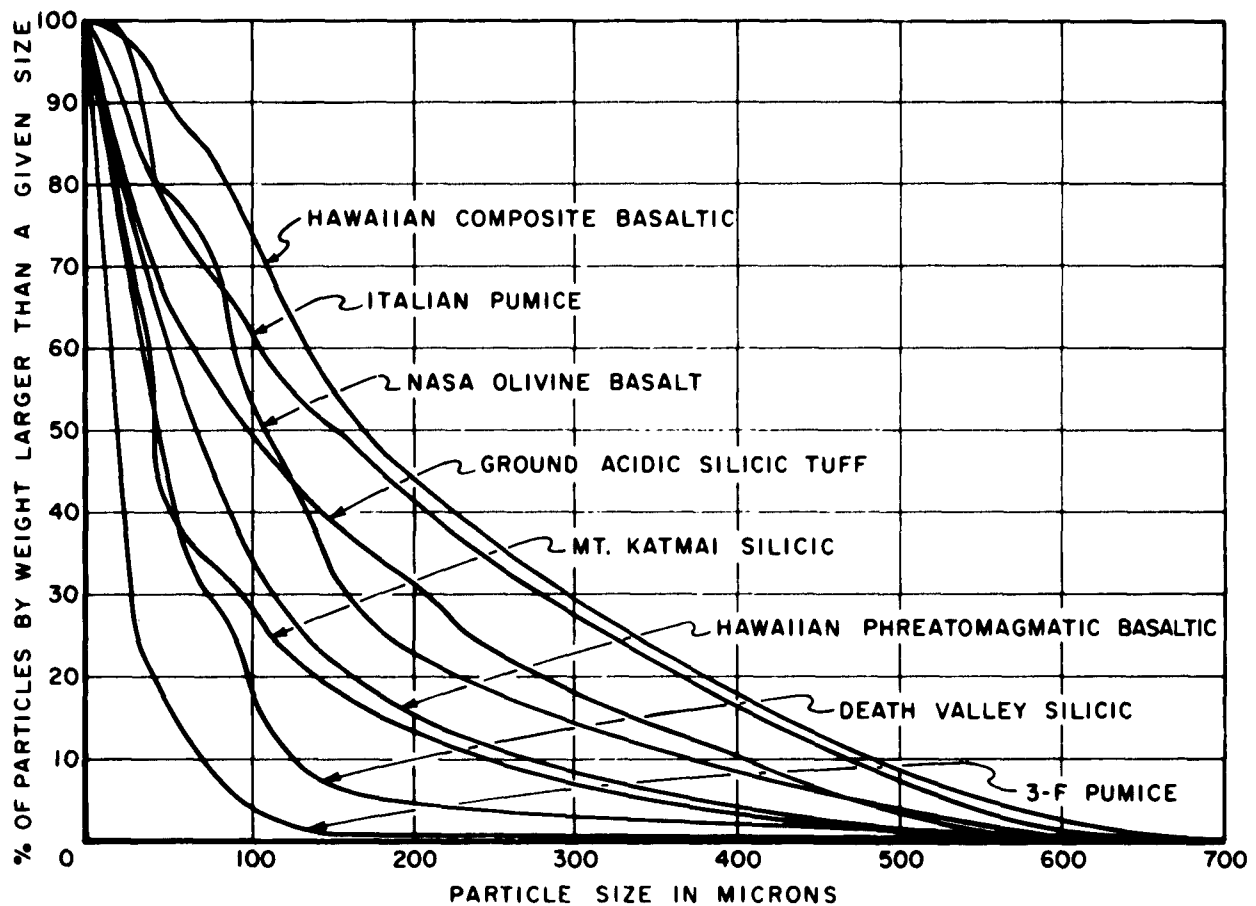


Figure 1. Comparative Particle Size Distribution

MICROSTRUCTURE OF THE DUSTS

The dynamic behavior of bodies in contact with each other is a function of their surface configuration and conditions. This is especially true for materials in a vacuum. Certain types of dust, by virtue of a larger ratio of surface area to particle size or by a greater chemical affinity for atmospheric gases, retain greater amounts of gas on their surfaces than others. Other dust types will have rough surfaces or projections that will tend to hinder the relative motion of the particle.

The photomicrographs which follow (Figs. 2 through 6) illustrate the microstructure of the dusts. For convenience, a scale showing divisions of 0.1 mm, and magnified appropriately, is included along the margin of the figures. All the photomicrographs were taken with polarized light.

Figures 2 and 3 illustrate the microstructure of the naturally-occurring silicic volcanic dusts. The 3-F pumice (Fig. 2) is composed of a vitreous material having a variety of shapes but generally smooth surfaces.

The Death Valley silicic dust resolves under magnification into two types of particles: transparent particles similar to the 3-F pumice, and translucent particles similar to the

others in size and shape. (The photomicrographs give a misleading impression as to particle size distribution, as may be noted by comparing Fig. 2 with Fig. 1.) It is entirely possible that the Death Valley dust from Tecopa was mixed with another silicic dust from near Sendal in an unknown amount. Since any given lunar area could very well be covered with silicic dust from two or more simultaneously operating sources producing slightly different dusts, this possibility of mixture was not considered to invalidate in any way the dust as a lunar soil model.

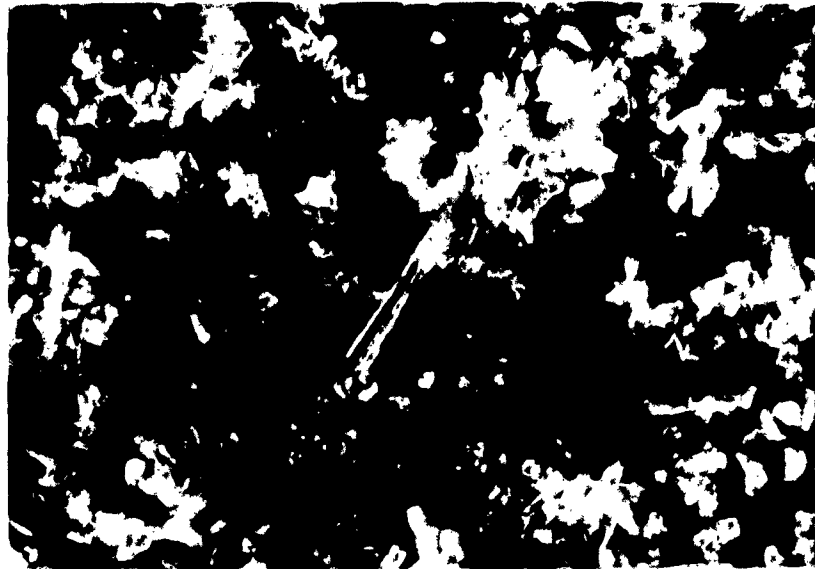
The Mt. Katmai dust is rather singular in its characteristics. This dust from the great eruption of 1912 spread a layer of fine dust all over the world and actually appreciably reduced the solar energy reaching the earth for many months (Ref. 20:355). Consequently, it is to be expected that this dust will be exceptionally fine; an examination under the metallographic microscope confirms this expectation (Fig. 3). However, the quantitative measurement provided by the sieve analysis indicates a generally coarser distribution of particles than either of the other natural silicic volcanic dusts. The fuzziness of the best picture obtainable provides a clue to help in resolving this apparent anomaly. The larger particles are apparently clumps of smaller particles rather loosely bound. Even the smallest particles observable at the highest magnification obtainable seemed to be aggregates of yet smaller particles. Consequently, the Mt. Katmai dust has a larger ratio of surface area to particle diameter than any of the other dusts tested.

The Hawaiian basaltic dust shown in Figure 4 also has many large particles formed by aggregates of smaller particles, but this aggregation is the result of weathering and results in a considerably stronger and denser bond than in the Mt. Katmai dust clumps. This Hawaiian dust was the densest dust tested. It also had the rather odd property of being moderately ferromagnetic, due to the presence of a large amount of $\text{Fe}_2\text{O}_3 \cdot \text{FeO}$. (The dust is brown, however, rather than black, as one would expect from magnetite.) Considerable organic matter (palm fibers, etc.) was found in this and a few of the other dusts during sieving. All but insignificant amounts were removed prior to testing the dust.

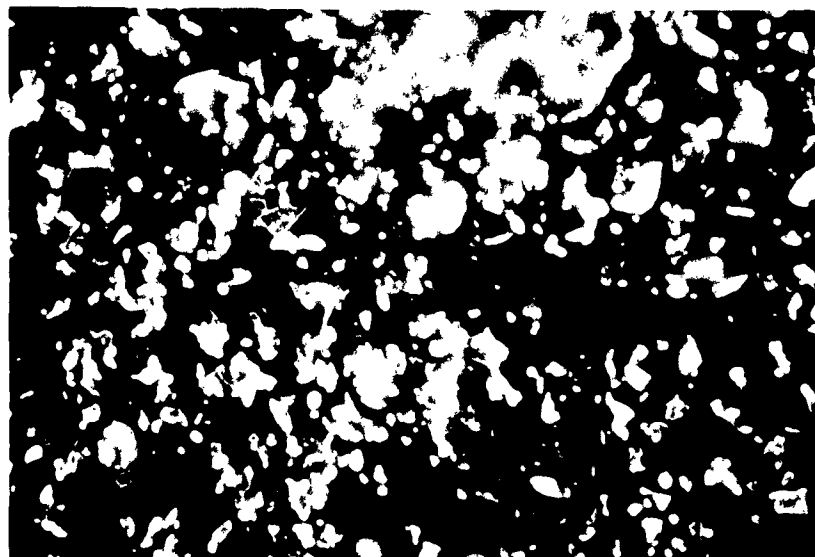
The ground dusts are all coarser than the dusts occurring in nature, as is apparent from Figure 1 and from the photomicrographs. The dust ground from a partly decomposed silicic acid tuff contained many pieces of an unidentified metallic mineral which had been imbedded throughout the tuff. These pieces were too few to affect the test and were not separated out. Both the rock dust and the associated mineral proved to be magnetic, indicating the mineral may be magnetite. The photomicrograph of the ground tuff (Fig. 4) reveals translucent shards with irregular shapes and both smooth and rough surfaces.

The Italian pumice and the acidic silicic tuff were dissimilar in appearance, but their dusts seemed to be quite similar, other than the color, and the lack of a stray mineral in the Italian pumice (Fig. 5).

The microstructure of the reticulite shown in Figure 4 (which, incidently, is the world's lightest rock at 0.03 gms/cc.) and the basaltic pumice shown in Figure 6 are identical despite the disparity in their age. On the strength of this identity (reticulite is simply extremely light basaltic pumice), the two were combined in a ratio of 58 parts reticulite to 42 parts basaltic pumice to form one pulverized basaltic dust for testing purposes (Fig. 6).



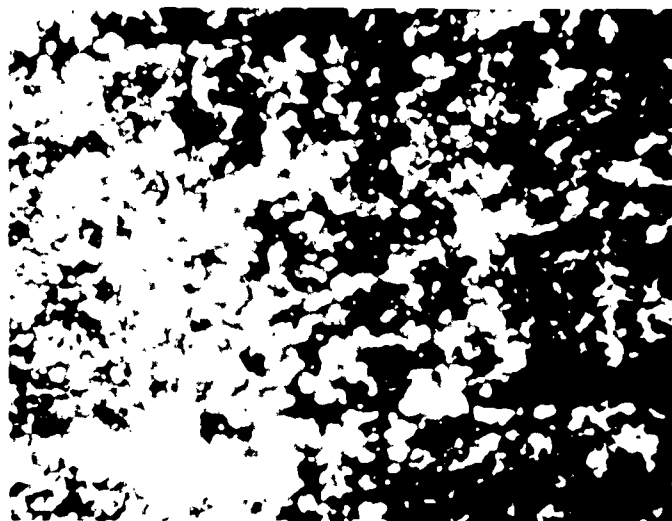
3-F Pumice (73.5 X)



Death Valley Silicic (73.5 X)

Figure 2. Natural Silicic Dusts of Volcanic Origin;
3-F Pumice and Death Valley Silicic

0.1 mm X 73.5 BETWEEN DIVISIONS

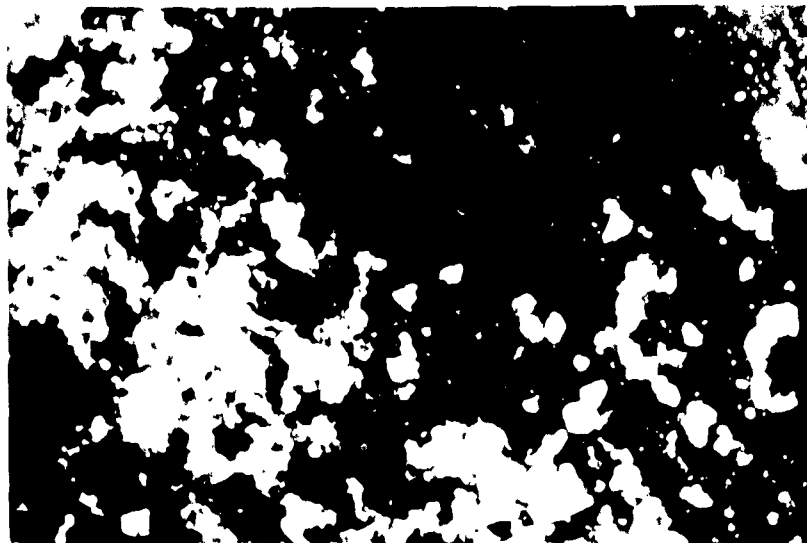


Mt. Katmai Dust (152.4 X)
from the eruption of 1912

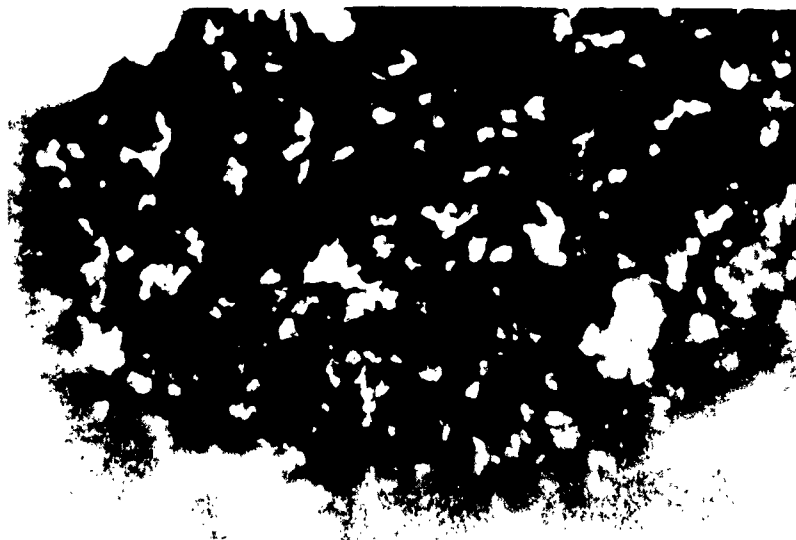
Figure 3. Natural Silicic Dust of Volcanic Origin from Mt. Katmai

152.4 X 0.1 AND 0.01 mm BETWEEN DIVISIONS





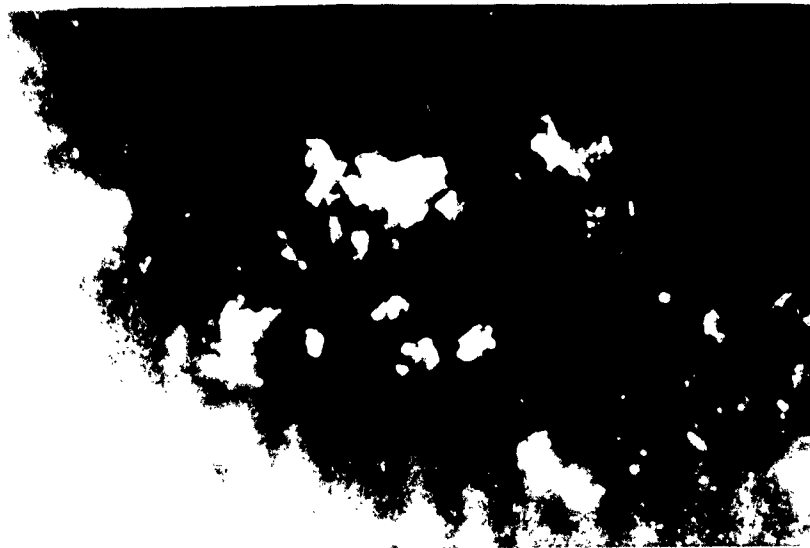
Hawaiian Basaltic Dust (70.7 X)
from the Phreatomagmatic Eruption of Kilauea, 1790



Silicic Acidic Dust (Ground Tuff) (70.7 X)
Ground from a Partly Decomposed Tuff from the So. Calif. Desert

Figure 4. Magnetic Volcanic Dusts

0.1 mm X 70.7 BETWEEN DIVISIONS



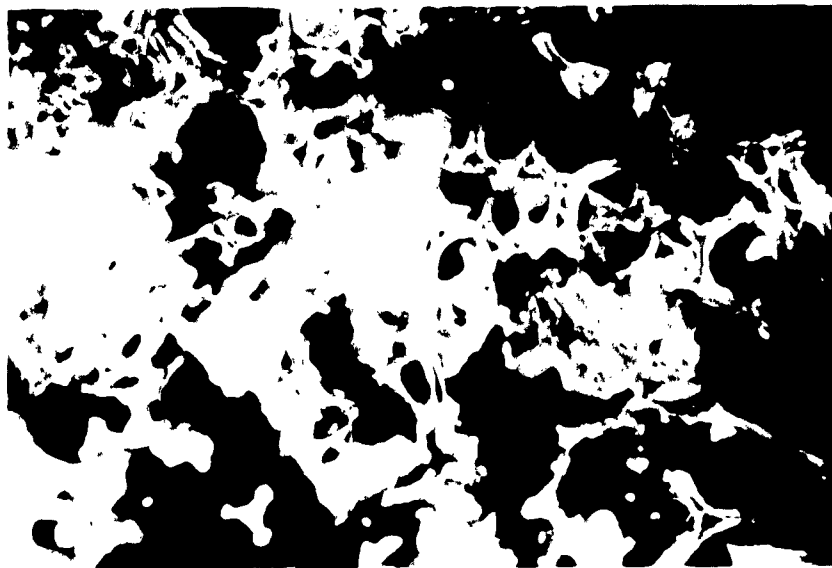
Ground Italian Pumic (70.7 X)



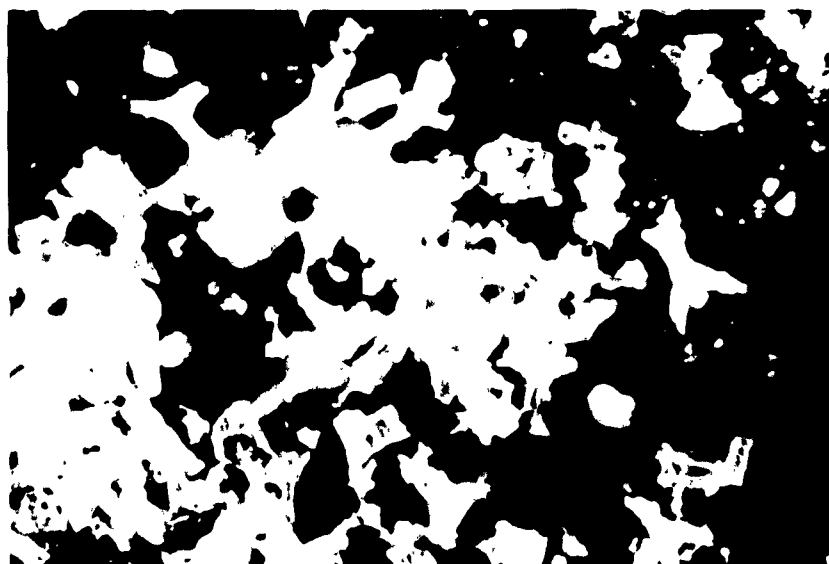
Hawaiian Basaltic Reticulite (70.7 X)
from Lava Fountains in Kilauea Volcano. Approx. 2500 yrs old.

Figure 5. Pulverized Dusts of Volcanic Origin

0 1 m m X 70 7 BETWEEN DIVISIONS



Pulverized Basaltic Pumice (73.5 X)
from the 1959 Eruption of Kilauea Volcano



Ground Hawaiian Basaltic Composite (73.5 X)
A mixture of Reticulite and Basaltic Pumice in a 57.9:42.1 ratio, by weight

Figure 6. Pulverized Hawaiian Basaltic Dusts

0.1 mm X 73.5 BETWEEN DIVISIONS

SECTION 3

THE TEST PROCEDURE

A thorough review of the experimental techniques used in making these impact studies is essential to understanding the results. The data suffers from the considerable uncertainty inherent in the study. The uncertainty does not invalidate the work, but it does require that the limitations of the information developed in this thesis be well understood if the results are to be applied successfully. All tests were made in the Flight Control Laboratory, Aeronautical Systems Division. The vacuum equipment was run by Environmental Division personnel.

THE TIME HISTORY OF THE DATA RUNS

The sequence of events for all of the data runs was essentially the same. Prior to the run, the dust was stirred up to remove the effects of any previous screening. It was then spread in a shallow pan and heated in an oven at between 250°F and 400°F for 2 hours or more to drive off water vapor and left in the hot oven over night. On the morning of the test, the dust was removed from the oven, placed in a special cannister 11 inches in diameter and 4 inches high, and mounted in a bell jar (Fig. 7). The dust was thoroughly stirred again to achieve homogeneity and leveled to a preselected depth. Steel balls 0.555 inches in diameter and 11.87 grams in weight were placed around the periphery of the wire mesh screen. The bell jar was then lowered and the roughing pump was started.

The diffusion pump was cut in near 0.08 mm Hg pressure, and the liquid nitrogen was started into the cold trap at about 0.025 mm Hg. A pressure of 1×10^{-5} mm Hg, which was the lowest that could be held without considerable fluctuation, was reached in approximately 3-1/4 hours. Pressure was held at 1×10^{-5} mm Hg for between 18 and 20 hours, during which time the adsorbed gas molecules on the dust-particle surfaces worked their way up through the dust and reached equilibrium with the gas particles in the bell jar.

During the evacuation of the bell jar and the long hold at vacuum, the cannister was vibrated to expose all the dust surfaces to vacuum and to prevent the escaping gas molecules from creating a metastable state of fluffed-up dust particles. The vibration was accomplished by a small solenoid mounted under the cannister, as shown in Figure 7. Vibration was held to a fixed schedule (3 seconds every half hour during hold and more often during pull-down) to avoid overheating the solenoid and to keep the degree of mechanical packing fairly constant for the different dusts. The amplitude of the 60-cycle vibration was just sufficient to be felt at the surface of a 3-inch-deep dust sample, but insufficient to produce up-welling or significant antinodal peaks and valleys in the dust surface. The dust was no longer vibrated after the first ball was dropped to avoid disturbing the craters.

After 18 to 20 hours of hold time, an electromagnet outside the bell jar (Fig. 7c) was used to pick up the first of the steel balls and maneuver it into a preselected position at the top of the jar. After the ball stopped spinning and rocking (due to friction with the wall during its passage up the side of the jar), it was released to drop with an impact force of between 0.619 and 0.561 inch-pounds of kinetic energy. The impact force varied by as much as 9.45 percent between tests, but the variance during any given test was no more than 3.9 percent.

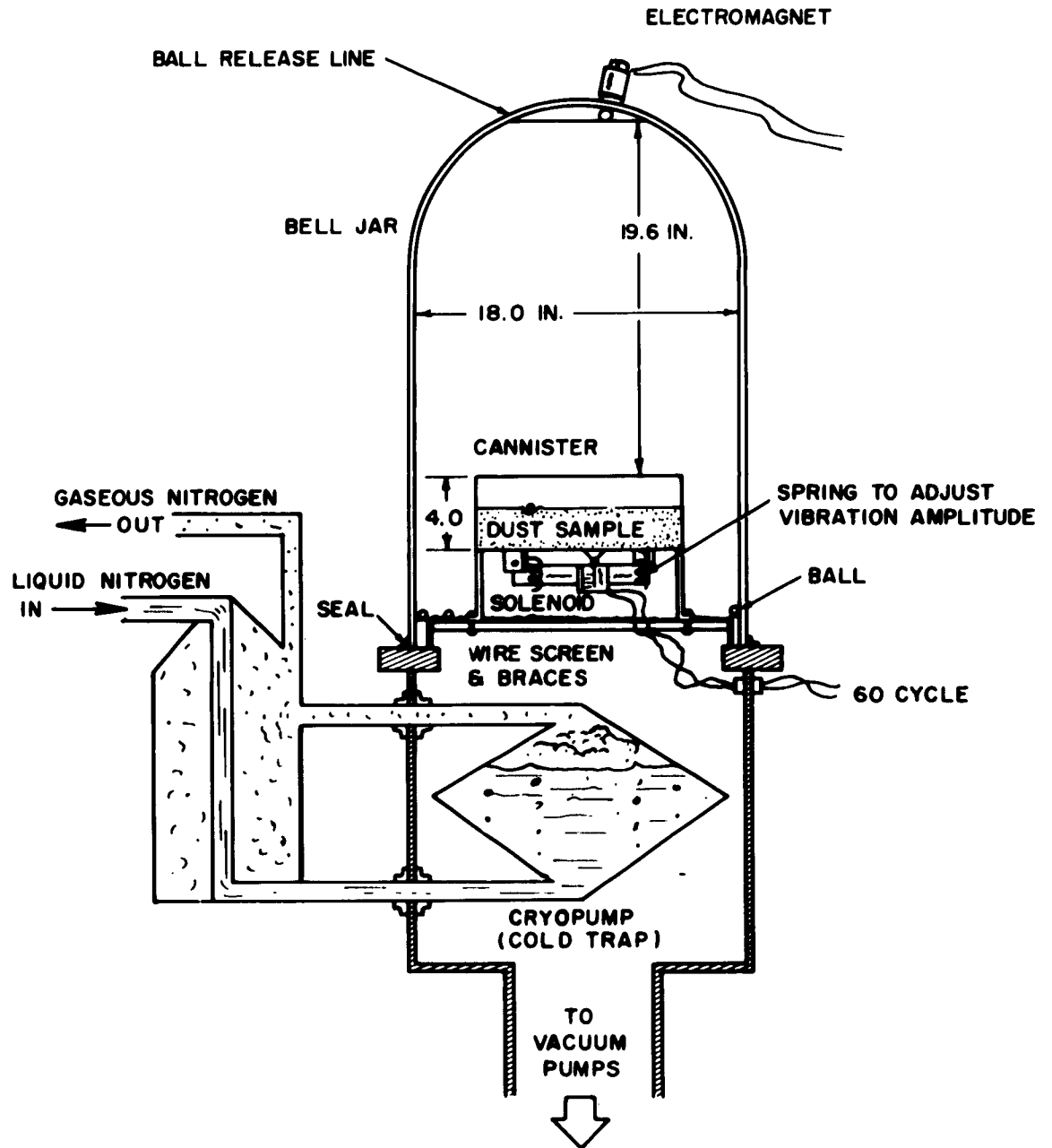


Figure 7a. Schematic Diagram of the Apparatus

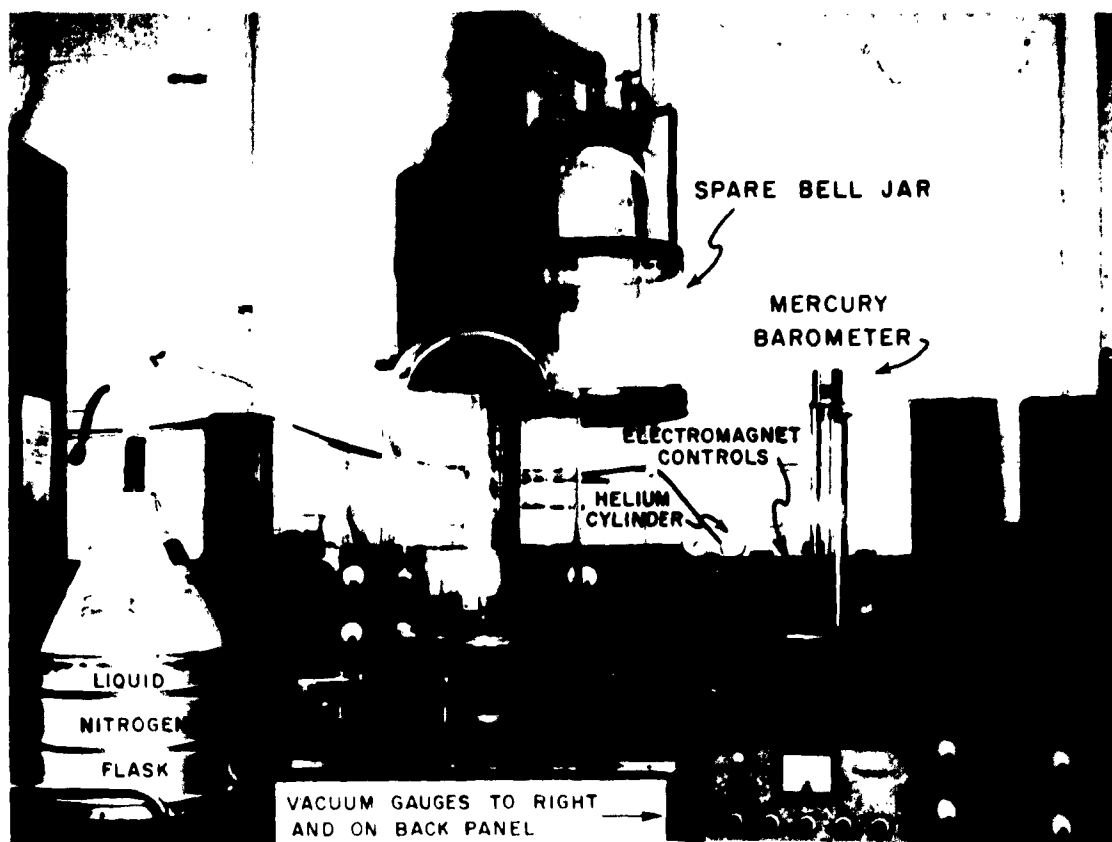


Figure 7b. Layout of the Apparatus

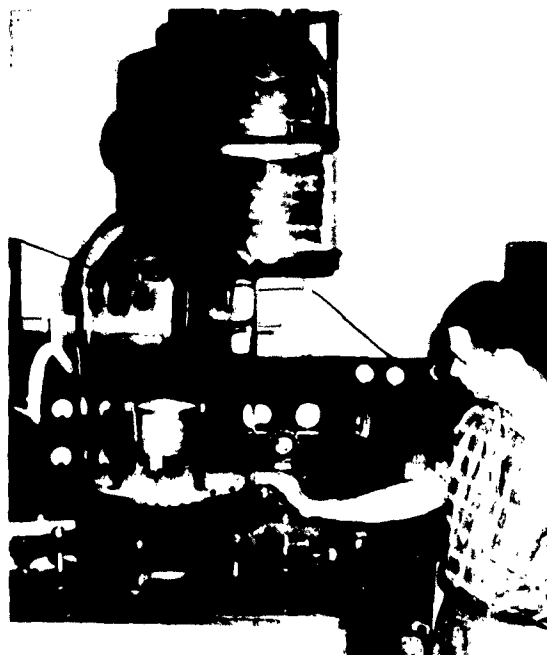


Figure 7c. Operation of the Electromagnet

A small amount of helium was then released into the bell jar to bring the pressure to 5×10^{-5} mm of Hg. This pressure was held for 2 hours until a new equilibrium was reached. The second ball was then dropped. Subsequent drops were made at 1×10^{-4} , 1×10^{-3} , 1×10^{-2} , 1×10^{-1} , 1, 10, and 100 mm Hg, and at ambient pressure. The hold times were 2 hours at 1×10^{-4} , 1 3/4 hours at 1×10^{-3} , 1 hour at 1×10^{-2} , 1/2 hour at 1×10^{-1} , 15 minutes at 1 mm Hg, 5 minutes at 10 mm Hg, and as fast as the pressure was established thereafter. Dry helium was bled in to adjust the pressure of the bell jar from 1×10^{-5} to 100 mm Hg, and room air was used thereafter.

After the last drop, the bell jar was removed and the craters were photographed and measured. When we discovered that removing the ball changed the shape of the crater, we measured craters with the balls intact.

THE VACUUM EQUIPMENT

As mentioned earlier, the pumping equipment consisted of a roughing pump, a diffusion pump, and a liquid nitrogen cryopump or cold trap. Higher vacuums could probably have been obtained with a shielded cold trap, or a cold trap using liquid hydrogen. An attempt to obtain higher vacuums by heating the bell jar glass with a wrap-around resistance heater did not prove successful due primarily to the unevenness of the temperature distribution on the jar (and possibly also due to the radiant heat effect on the unshielded cryopump).

The vacuum gauges used varied somewhat from run to run. All pressures of 10^{-3} mm Hg and lower were measured on a Distillation Products, Inc., ionization gauge. Pressures from 10^{-2} to 10 mm Hg were usually measured on the thermocouple section of the Consolidated Vacuum Corporation Type GIC-100 vacuum gauge. A National Research Corporation Alphasatron Type 510 high-vacuum gauge was used occasionally to measure pressures between 10^{-2} and 10^{-1} mm Hg, and an NRC Type 706 thermocouple gauge was used on two runs to measure pressures from 10^{-3} to 1 mm Hg. All pressures from 1 mm Hg to 10 mm were measured on a Bourden tube. At pressures from 10 mm Hg to ambient, a Hass Brothers Instrument Co. mercury barometer was used. Figure 7b shows the layout of the equipment.

METHODS OF MEASURING THE EFFECTS OF IMPACT

Preliminary tests of the lunar dust models revealed that we could describe the effects of impact on the dust in a meaningful qualitative manner, but that quantitative measurements would also be desirable. Three measurements were developed: depth of penetration (DP), crater rim diameter (CRD), and maximum diameter of crater (MDC).

The depth of penetration of a given dust refers to the penetration of the ball relative to the mean surface level of the surrounding dust. The vertical distance from a fixed reference plane to the top of the ball is added to the ball diameter. From this value, we subtracted the average of several vertical distance measurements from the reference plane to the undisturbed dust surface immediately surrounding the ball to obtain the DP.

The crater rim diameter is the diameter from rim-to-rim of the crater, as measured from the highest contour line above the dust (the crater summit). In the case of the fine dusts at high vacuum (except for the Mt. Katmai dust) and the coarser dusts, this value is an average measurement: the average of the widest, narrowest, and intermediate diameters of what may have been an elliptical or irregularly-shaped crater.

The maximum diameter of the crater could not be measured for all the dusts at all vacuums; it is shown for only a few of the dusts. The craters, in these cases, had a maximum diameter, but they were either poorly defined, coincided with the crater rim diameter, or were otherwise unsuceptible to measurement. In some dusts, the MDC indicates the limit to which the dust surrounding a crater was distorted by the impact, and in other dusts, it indicates the limit to which the larger chunks of dust travelled when thrown out of the crater. The MDC, like the CRD, was often the average of several measurements.

THE CALIBRATION AND CHECK RUNS

A series of calibration and check runs was devised and executed to control the variables of this experiment to as great an extent as is possible in a time-limited study of this magnitude, and to validate the data. Nine series of runs were made, some with three or four runs, mostly before, but also between and after the data-gathering runs-for-the-record. These runs checked the influence of hold time at vacuum, calibrated the influence of the cannister wall and the pan position, and checked the influence of a different residual atmosphere. Data from these runs provided a basis for estimating the data scatter.

Unfortunately, because of time limitations, only one dust could be used for most of the calibration and check runs. The Death Valley silicic was chosen because it was in ample supply. The results of the calibration and check runs, therefore, are only specifically valid for the Death Valley silicic dust. Where experience indicated that the results could or should be applied to the other dusts, the values were applied with reservations. However, in order to err on the side of conservatism, the correction factors developed in the runs were not applied to the other dusts.

Influence of Hold Time at Vacuum on Crater Parameters

The question of how long to hold the system at a given level of vacuum to establish equilibrium is fundamental to the entire experiment. To establish proper hold times, a series of experiments was conducted at two levels of vacuum and various hold times. These experiments were made with the Death Valley silicic dust at a depth of 3 inches. One experiment (curve C in Figure 8) was made in shallow dust, and the data was corrected to a 3-inch depth because much of the Death Valley silicic dust was lost in a fountaining incident while the cannister was being pumped down to vacuum.

CRD and DP were measured after hold times of 5 minutes, 15 minutes, and 60 minutes at 10^{-2} mm Hg vacuum. The time was counted from the time the system reached the hold pressure, rather than from the time the pumps were started. The results, presented in Figure 8, show the average of several drops at each hold time. These data were inconclusive, but, allowing for the data scatter, they at least indicated that the CRD and DP had probably ceased their variation at the chosen hold time of 1 hour.

On the other hand, measurements made on the same dust at 5×10^{-6} mm Hg show conclusively (Fig. 8) that the characteristics of the dust had stopped changing after some 6 to 10 hours at vacuum. The measurement made in shallow dust and corrected to a 3-inch depth fails to lie on the plotted line. Even with correction for data scatter, this illustrates the limitation of (a) the data scatter estimate, and/or (b) the dust shallowness correction technique. It does not indicate an actual dip in the curve.

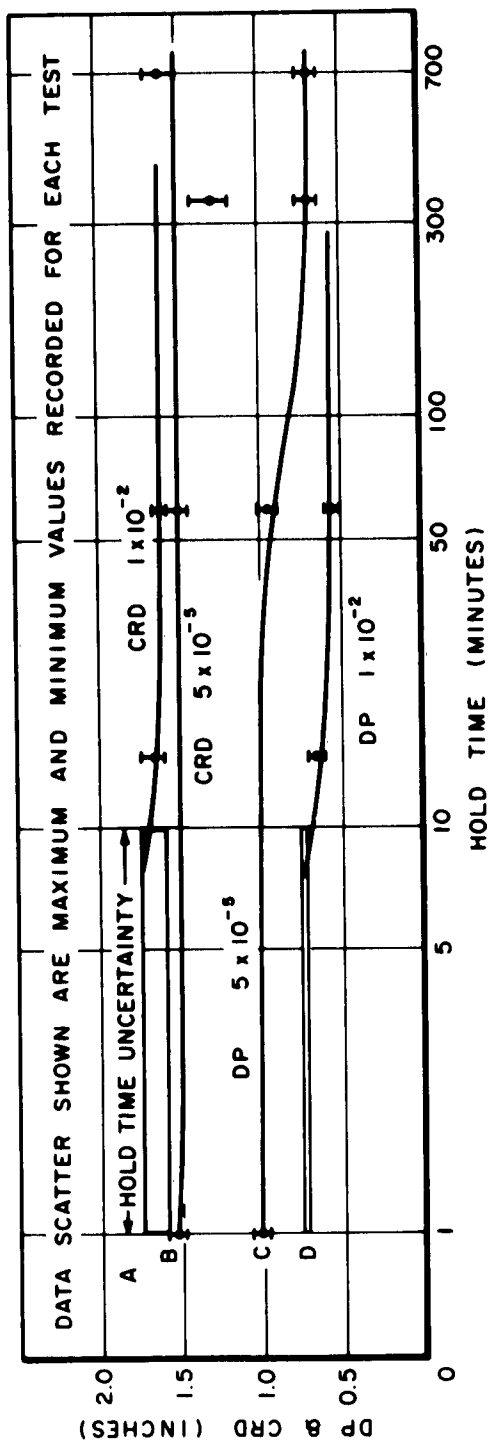


Figure 8. Effect of Hold Time on Depth of Penetration and Crater Rim Diameter for Death Valley Silicic Dust at 1×10^{-2} and 6×10^{-5} mm Hg

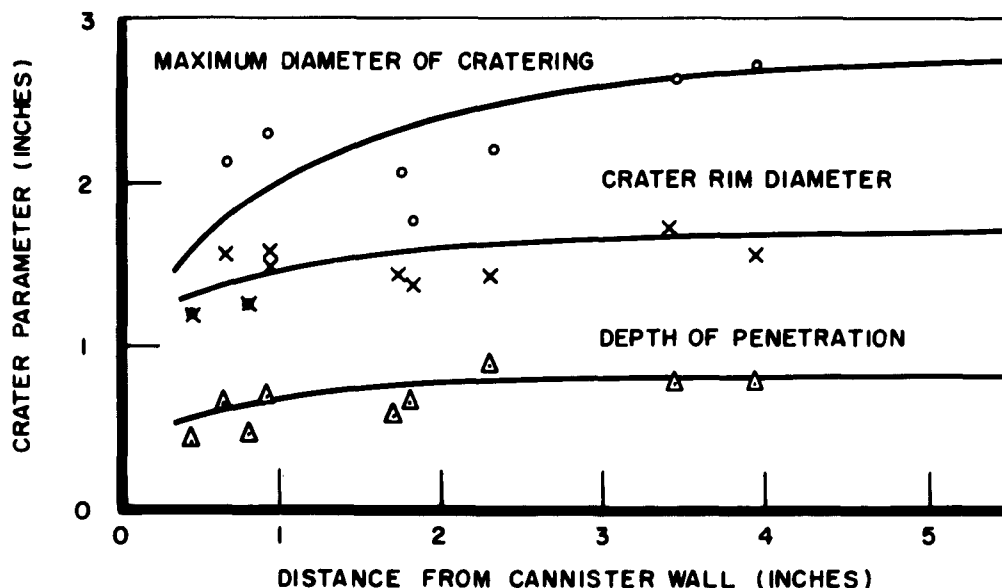


Figure 9. Variation of Crater Parameters with Distance from Cannister Wall

The hold times were derived by the following arguments: (1) the bigger the jump between the established pressure and the preceding pressure, the longer the hold time required to re-establish equilibrium; (2) the lower the pressure, the slower the gas molecules move through the dust from top to bottom, and hence, the longer the hold time required.

Thus, although 10 hours might be required to establish equilibrium when reducing pressure to 5×10^{-5} mm Hg from ambient, approximately 2 hours would be required to establish equilibrium at 5×10^{-5} mm Hg from a pressure of 1×10^{-5} mm Hg. We admit, however, that the hold times selected have not been really confirmed by the check runs; at best, we can say that they were not proved faulty.

Influence of Cannister Wall on Crater Parameters

An experiment was made with the Death Valley silicic dust at a 3-inch depth to determine the effect of the cannister wall on the crater parameters. The experiment was run at 10^{-1} mm Hg with a 3 1/2-hour hold time. The results are shown in Figure 9.

Factors for correcting DP and CRD values obtained for the Death Valley dust for distance from the wall were prepared and used to correct the readings at 10^{-1} mm Hg. We decided to ignore the data for any ball that was dropped closer than 2 inches to the wall. This decision proved itself correct many times by eliminating otherwise maverick points from data plots.

Influence of the Depth of Dust on Crater Parameters

For comparing the behavior of the different dusts, all dusts should be tested at the same depth. Unfortunately, some dusts were available in greater quantity than others. Rather than run the risk of invalidating all the data by possible bottom-of-the-pan effects, we tested most of the dusts at their maximum depths. A group of dusts in good supply, however, were tested at a common depth of 2.2 inches. The calibration was run, also, because it was intrinsically desirable to find the effect of shallowness on certain dusts.

For these tests, the Death Valley silicic and the Hawaiian phreatomagmatic basaltic were used. The Death Valley silicic was run at 5×10^{-6} mm Hg with a 1-hour hold at depths of 1.5 and 3.0 inches. The Hawaiian phreatomagmatic basaltic was run at 1×10^{-6} mm Hg, with a 255-minute hold, at a depth of 1.1 and 2.2 inches. On each run, 4 or 5 drops were made, averaged, and compared. The results were converted into percentage deviation from normal for a given percentage reduction in dust depth. A linear extrapolation was used to adjust the values obtained at 2.2 inches for the reference dusts for comparison with those tested at shallower depths. This extrapolation of the effect of shallowness is shown in Figure 10. These values are not to be taken too seriously, as there is no reason to believe the effects of dust shallowness are linear. The effects, however, tend in the direction indicated. Why two dusts have such divergent behavior with variation of depth is not known.

Influence of Position in Pan on Crater Parameters

Whether a ball is dropped in the 9 o'clock, 12 o'clock, or 6 o'clock position should make no difference in the DP, CRD, and MDC measurements. The solenoid was mounted slightly off center, however, and the walls of the cannister are more rigid in some places than in others, so the dust in the cannister was slightly more compacted in some areas than in others. By studying all the calibration and check runs, we were able to assign qualitative correction factors to the results to compensate for this effect in drawing the curves. When a DP seemed too large in relation to the other DP's in a given test, we deviated from the value if it represented a ball dropped in a known "soft" area. On the other hand, if the DP was from a known "hard" area, the plotted curve must take that point into account. This correction was used in plotting Figures 11 and 12.

Influence of a Different Residual Atmosphere on Crater Parameters

As was mentioned previously, air was pumped out of the bell jar in all the runs, till a vacuum of 10^{-6} mm Hg was achieved. Helium was used to increase pressure up to 100 mm Hg. Room air was bled in to increase pressure from 100 mm Hg to ambient. To discover the effect, if any, that a different type of adsorbed gas molecule would have on the crater parameters, we made a control run with another type of atmosphere.

The Death Valley silicic dust was tested using an atmosphere of carbon dioxide and hydrogen in a ratio of one part to ten by volume. These particular gases in this particular ratio were chosen only because the gases are readily available and this ratio might possibly exist on the moon (hydrogen from the sweep-out of interplanetary space and solar proton and electron bombardment, and carbon dioxide from volcanic emission and retention over many millennia. Refs. 6:1606, 15:135.).

The run was begun as usual with room air in the bell jar. The pressure was reduced to between 1×10^{-4} and 1.1×10^{-5} mm Hg for 2 hours and the dust was vibrated to reduce the amount of air molecules retained on the dust. The 1:10 ratio of CO_2 and H_2 was then introduced at a pressure of 1 mm Hg. The new atmosphere was maintained in the bell jar at 1 mm Hg for 1 hour to allow the carbon dioxide and hydrogen molecules to displace the oxygen and nitrogen molecules retained on the dust surfaces. (The pressure was maintained at 1 mm Hg to reduce the possibility of fire hazard inherent in working with hydrogen.)

The vacuum was then increased to 1×10^{-6} and maintained between 9×10^{-6} and 1×10^{-5} mm Hg for the standard hold time (exactly 19 hours and 45 minutes, in this case). After the first drop, additional gas was introduced to raise the pressure to 5×10^{-5} mm Hg.

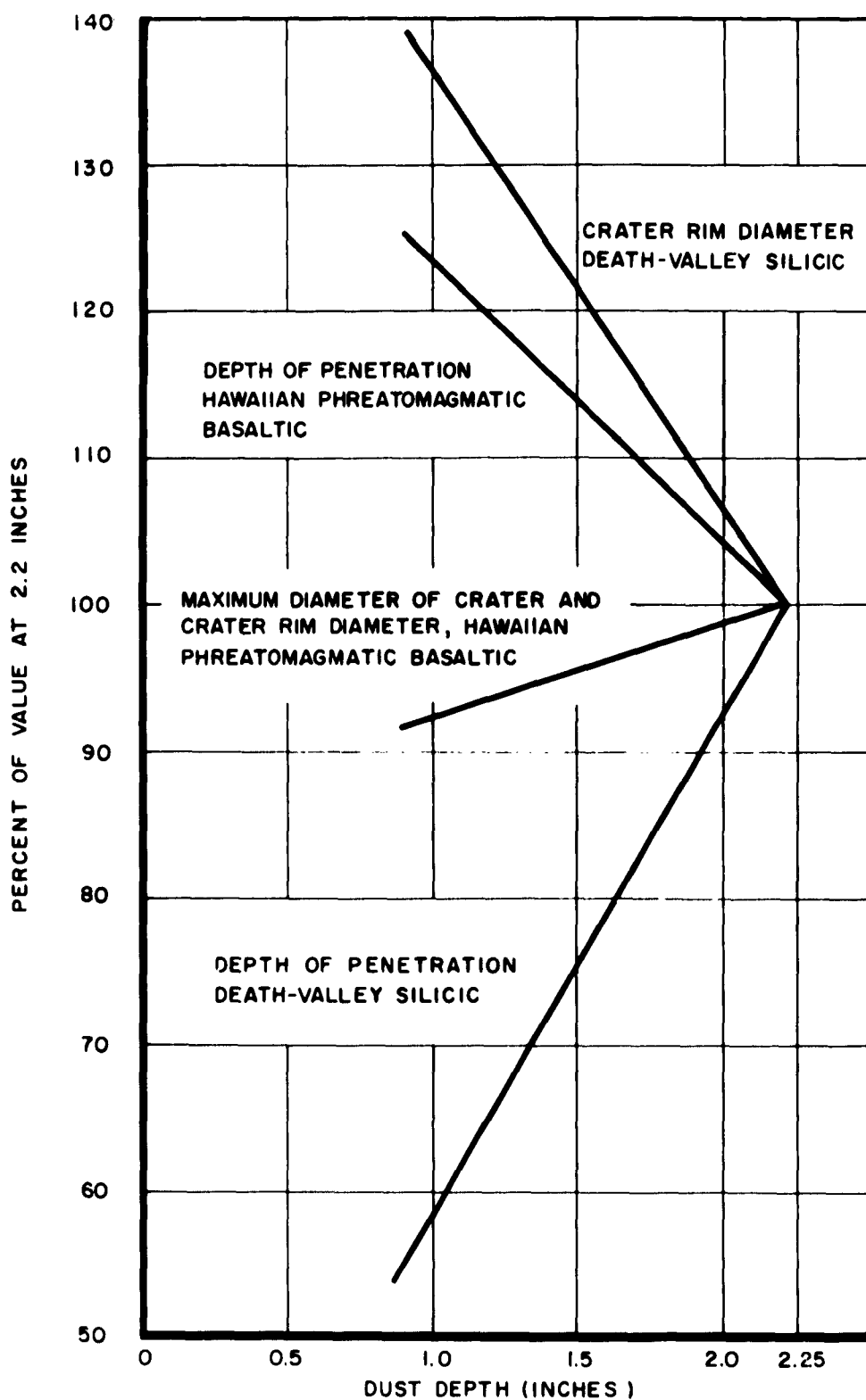


Figure 10. Effect of Dust Shallowness (Linear Extrapolation)

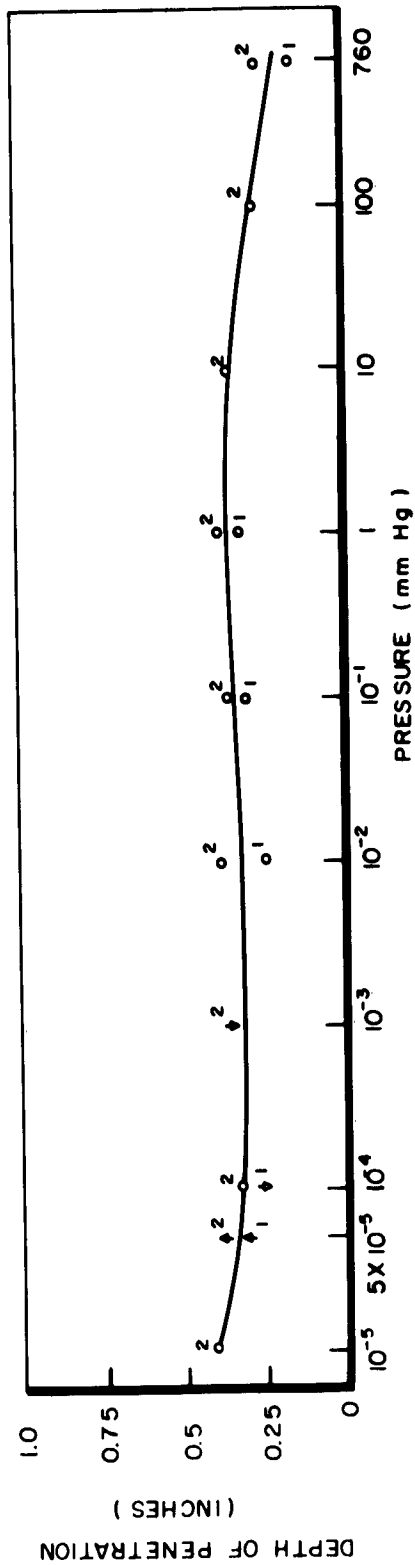


Figure 11. Depth of Penetration, Death Valley Silicic Dust, 2.2 Inches Deep

CODE .
CORRECTIONS FOR LOCAL DENSITY
♦ POSSIBLE DIRECTION OF AVERAGE VALUE
▲ PROBABLE DIRECTION OF AVERAGE VALUE
1 RUN OF 2 JUNE 1961
2 RUN OF 6 JUNE 1961

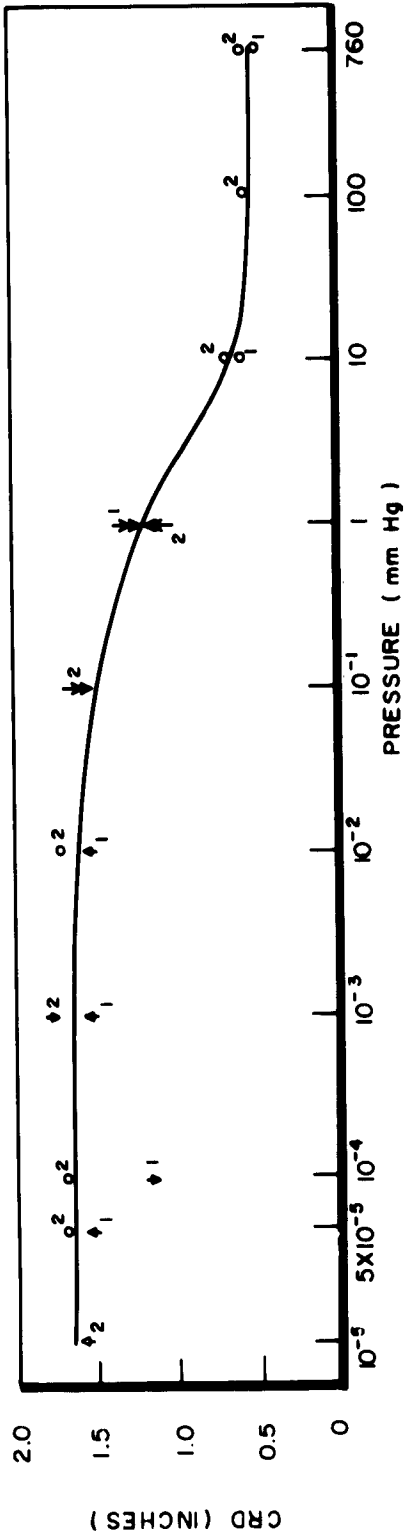


Figure 12. Crater Rim Diameter, Death Valley Silicic Dust, 2.2 Inches Deep

The carbon dioxide - hydrogen mixture was added to increase the pressure for subsequent drops to 1 mm Hg. At higher pressures, increases were made by adding pure carbon dioxide. The hold times and pressures at which balls were dropped were identical to all the other data runs.

The results of this run are compared to the average of the two Death Valley silicic runs made with the usual atmosphere in Figures 13 and 14. It should be noted that the new atmosphere seemed to lower both DP and CRD values. The apparent decrease is comparable to the difference in runs 1 and 2 for the dust at standard atmosphere, as shown in Figures 11 and 12.

Discussion of the Data Scatter

In any experiment of this nature, there is bound to be considerable data scatter. In a second run, a given data point might measure several points off the value obtained in the first run. To not be misled into drawing a curve through stray points that might prove to be only maximum or minimum variations from an average value, something should be known about the scattering inherent in the data.

Data-scatter information was drawn from all the check runs. In a certain check run, for instance, five balls might have been dropped at a given pressure and hold time. To find the data-scatter value, we might average the values for 4 of the 5 balls (if one had landed too close to the wall) and find the maximum and minimum deviations from the average. The deviations from average would be translated into percentage deviations and compared with other percentage deviation figures, similarly obtained. In this manner, we derived data-scatter values for the Death Valley silicic and phreatomagmatic basaltic dusts. These values are shown as Table 3.

It must be emphasized that the assignment of these values is somewhat arbitrary since the actual data scatter for the actual hold times for each of the pressures was not measured. That these values are estimates based on samples of the whole population of test conditions does not destroy their utility, since some idea of the data scatter is better than no idea at all. It should be added that the value of scatter assigned to a dust seemed to be commensurate with the amount of study the dust received.

Unfortunately, time limitations precluded getting any data-scatter figures for most of the dusts. In these cases the curves of variation of a given crater parameter with degree of vacuum were fared smoothly close to the plotted points, in general conformity both with the other, better-established curves, and with the estimated data scatter for that dust.

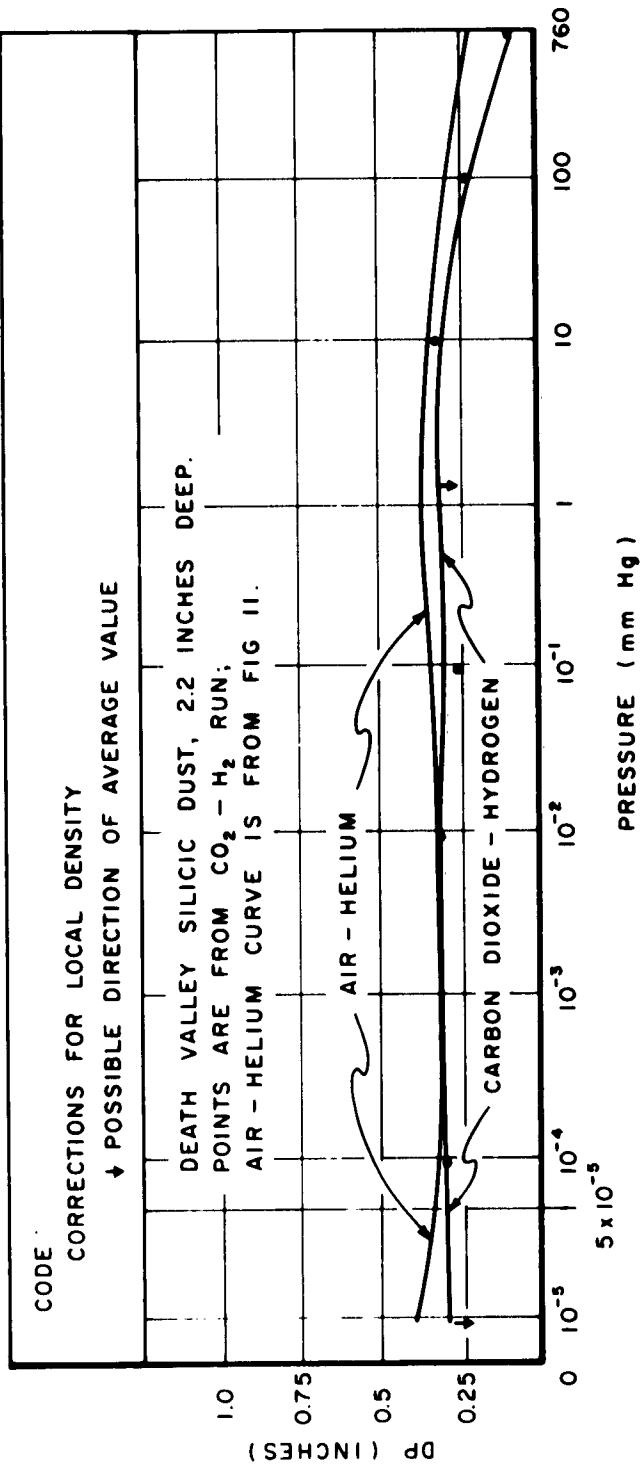


Figure 13. Comparison of Depth of Penetration in Air-Helium Atmosphere with Carbon Dioxide-Hydrogen Atmosphere

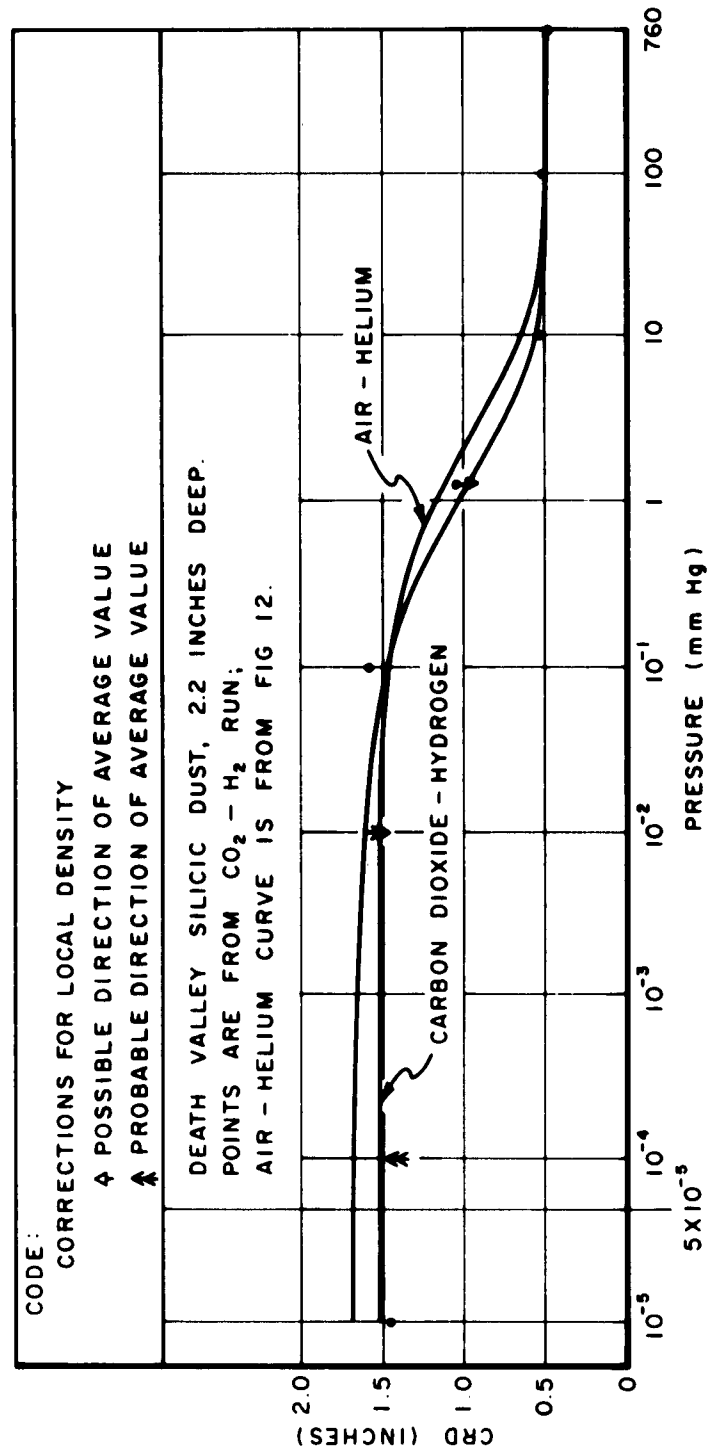


Figure 14. Comparison of Crater Rim Diameter in Air-Helium Atmosphere with Carbon Dioxide-Hydrogen Atmosphere

TABLE 3

ESTIMATED DATA SCATTER

Dust	Possible Variation of Average from Single Value		
	Depth of Penetration	Crater Rim Diameter	Maximum Diameter of Crater
Death Valley Silicic	Up to $\pm 22\%$ of nominal; usually $\pm 10\%$	Up to $\pm 27\%$ of nominal; usually $\pm 10\%$	Not measured
Hawaiian Phreatomagmatic Basaltic	$\pm 6\%$ of nominal	$\pm 9\%$ of nominal	$\pm 12\%$ of nominal

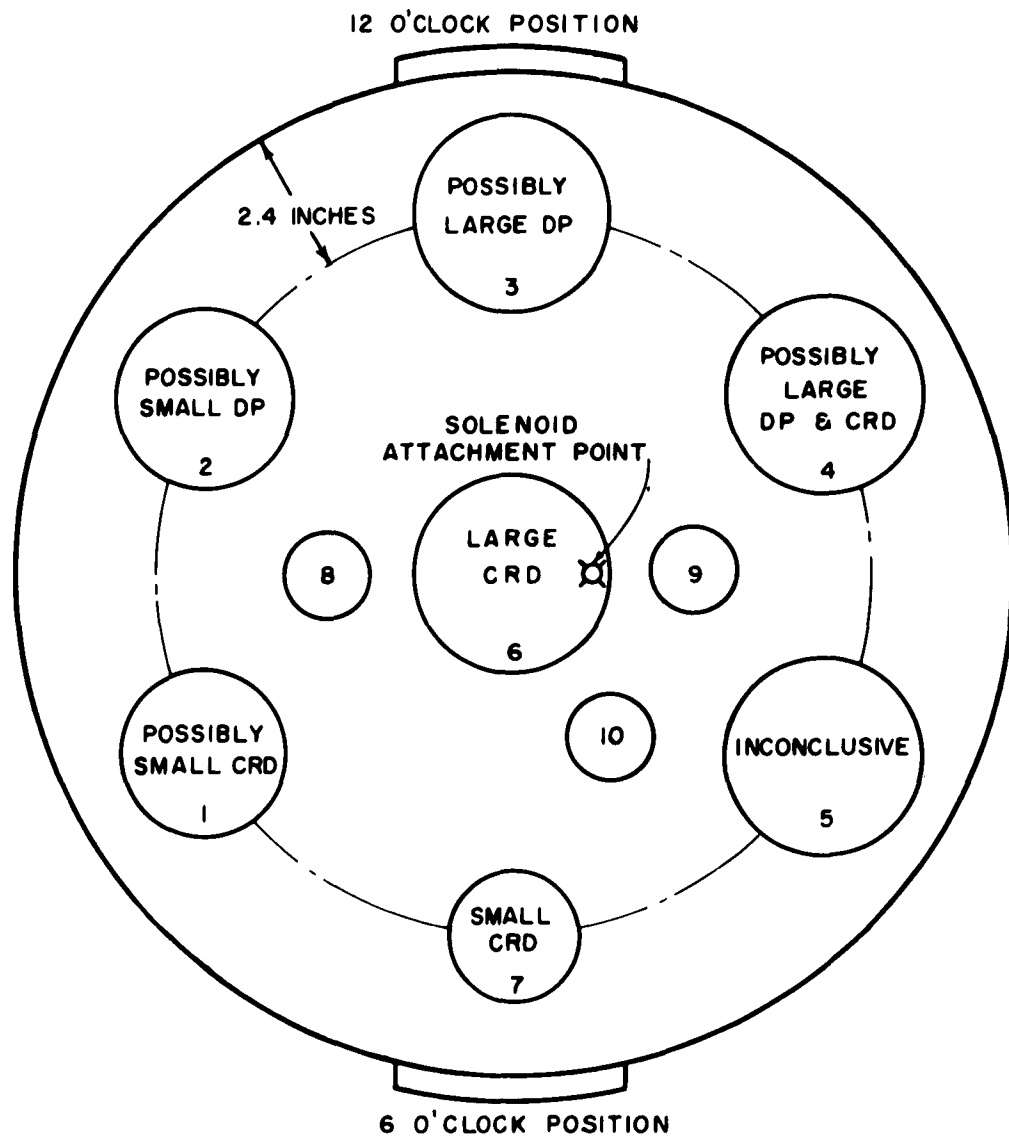
There are several reasons for the data scatter, probably operating simultaneously. The height from which the balls were dropped varied causing the kinetic energy to vary as much as 3.9 percent between drops in the same test. The slight spin or small horizontal velocity component that a ball might receive when released by the electromagnet could cause some scatter in the data. The dust density was somewhat uneven, as mentioned previously, due to the dynamics of the vibration imposed. Measurement errors were inevitable, since the precise summit line for the CRD, or the point at which the crater stops and the relatively undisturbed dust begins for the MDC, was difficult to estimate for some of the craters. The DP was probably the most unreliable measurement because the dust tended to develop small local height variations both because of imperfect leveling techniques and because of the vibration during the runs.

There is one major source of error that was not checked quantitatively: the effect of one drop on the craters made by previous drops. Certainly the shock from the impact of the ball was transmitted through the dust. This shock would sometimes manifest itself by cracks spreading out from the new crater or by slight distortions of the surrounding craters. After considerable trial-and-error, a pattern was developed for dropping the balls that appeared to leave sufficient margin between the balls so that the successive impacts had little or no effect upon the preceeding craters. This pattern is shown in Figure 15.

As a concluding remark to this part of the discussion, it should be pointed out that, insofar as is known, no other experiment studying dust behavior in a vacuum has investigated all the variables influencing the results. Neither has any experiment been carried out with such a variety of dusts or on such a large scale. (Grumman is beginning a large-scale experiment with four types of soils, but only one could be considered a lunar dust model.)*

* Telephone conversation 1 May 1961 and letter 21 June 1961 with Messrs J.D. Halajian and R. Stewart, project engineers, Grumman Aircraft Engineering Corporation, Bethpage, New York.

BALLS 8,9,10 WERE PLACED IN
LARGEST AVAILABLE SPACES
REMAINING AFTER DROP 7



DIAMETER OF CIRCLE INDICATES MAXIMUM
DIAMETER OF CRATER GENERALLY ENCOUNTERED
AT PRESSURE ASSOCIATED WITH THAT DROP
NUMBER

Figure 15. Ball Drop Pattern and Effect of Local Density Irregularities

SECTION 4

DISCUSSION OF THE TEST RESULTS

Because of the various uncertainties associated with the experiments, much of the data must be regarded as preliminary and much of the discussion must be so qualified. Nevertheless, certain principles and trends are well enough established by this study to be considered as documented fact. Many of the results are amenable to graphic display and others to photographic illustration. The variation of impact parameters will be shown for each dust and compared with the results from other dusts. Possible explanations for these results will be examined. Finally, the meaning of the results will be studied.

VARIATION OF IMPACT PARAMETER WITH DEGREE OF VACUUM

The cratering effects of all dusts were determined and results were photographed. Values for each were then plotted. Photographs of the cratering effects are presented in Figures 16 through 20 and plots in Figures 21 through 28.

Death Valley Silicic

The dust which received the most study was the Death Valley silicic. As might be expected, it also has the largest data scatter (Table 3) and hence the largest uncertainty factor assigned to interpreting its results. Figures 11 and 12 showed the variation of impact parameters with degree of vacuum. Generally speaking, the shape of the curve is correct, but the actual values the curve shows are uncertain by the amount of the known data scatter. This is true of nearly all the dusts tested.

The maximum diameter of the crater for the Death Valley dust proved too difficult to measure. Figure 16 shows the balls and their craters at the finish of the first of the two data runs made with the standard atmosphere on the Death Valley dust. It is apparent why no MDC measurements were made.

The ball drop pattern shown in Figure 16 is not the standard pattern established for subsequent data runs and illustrated in Figure 15. For this run, the balls were dropped at the following pressures: ball one, 1×10^{-5} mm Hg; ball two, 5×10^{-5} mm Hg; ball three, 1×10^{-4} mm Hg; ball four, 1×10^{-3} mm Hg; ball five, 1×10^{-2} mm Hg; ball six, 1×10^{-1} mm Hg; ball seven, 1 mm Hg; ball eight, 10 mm Hg; ball nine, 760 mm Hg. Craters 1, 4, and 8 were not used because the balls were dropped too close to the canister wall.

The craters made at the higher vacuums (one through six) are generally shallow and poorly defined, with irregular and rough interiors. Several dust clumps lie in or about the high-vacuum craters. Apparently, the dust particles cohere at high vacuum, but move independently of each other at lower vacuum to form a symmetrical, smooth crater (crater 7 of Fig. 16). At near ambient pressure, there is little cratering, and at ambient pressure (nine) the ball simply dents the surface of the dust.

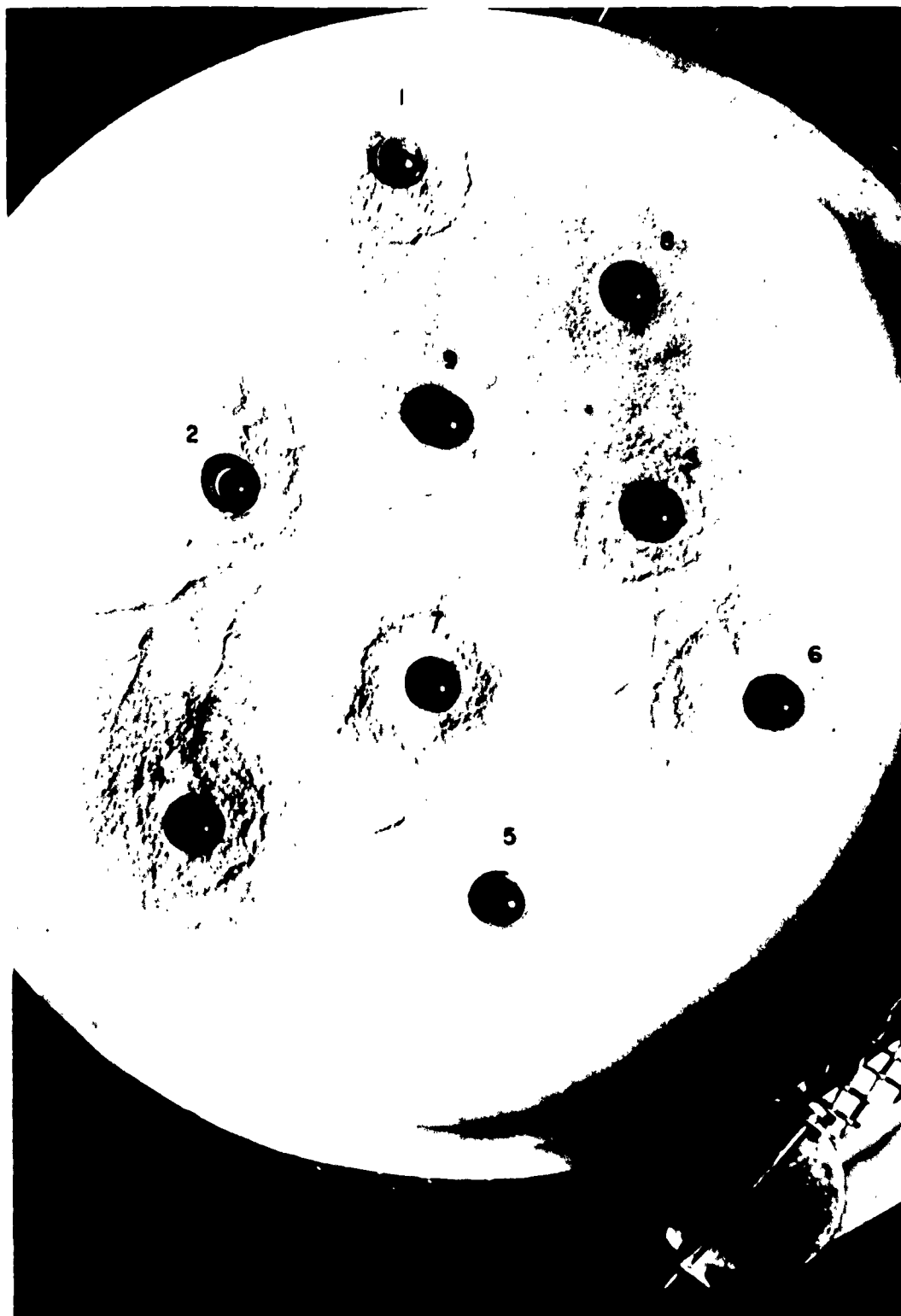


Figure 16. Cratering Effects of Death Valley Silicic Dust at Various Pressures with a Depth of 2.2 Inches



Figure 17. Cratering Effects of Hawaiian Phreatomagmatic Basaltic Dust at Various Pressures with a Depth of 2.2 Inches

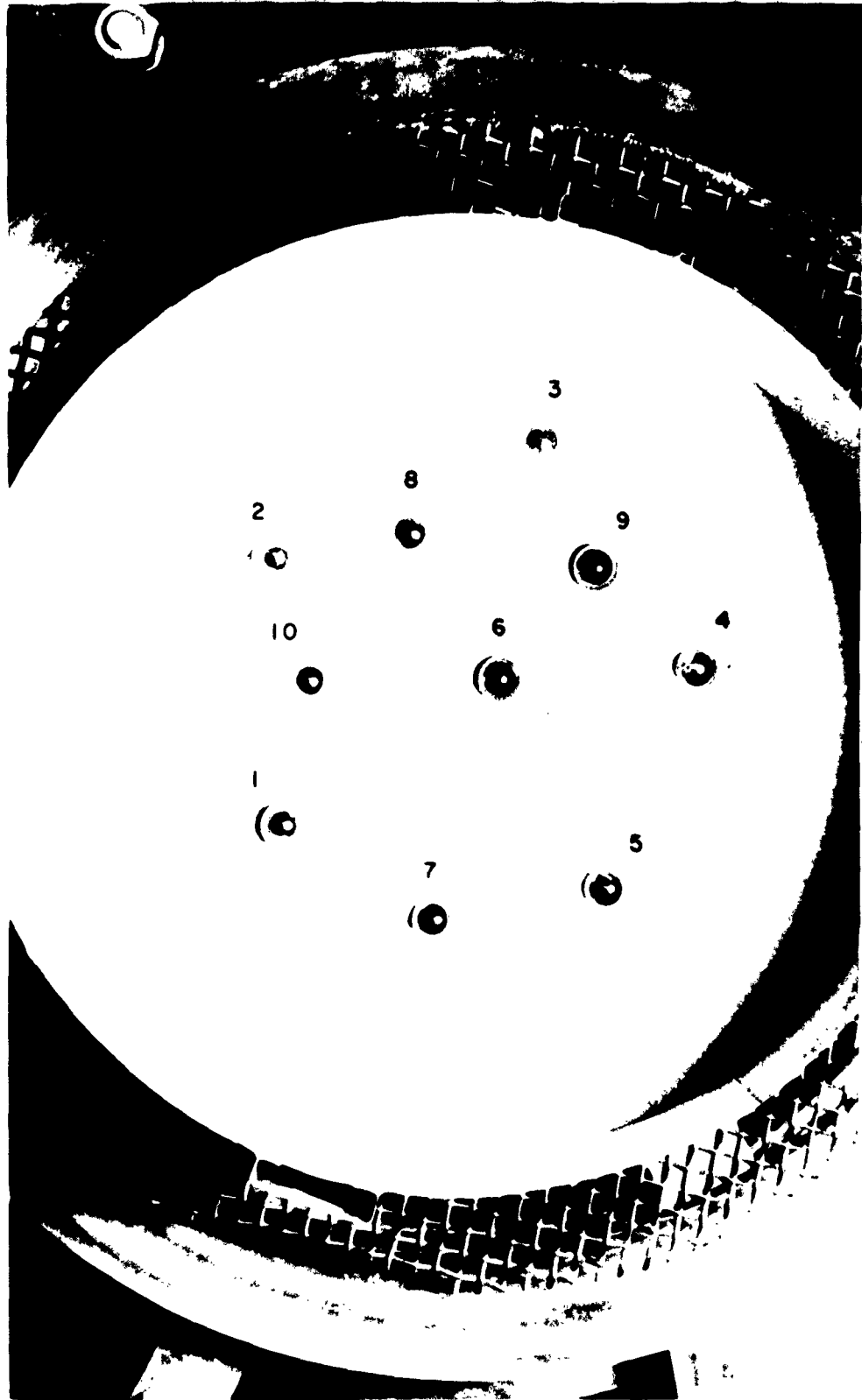


Figure 18. Cratering Effects of 3-F Pumice Dust at Various Pressures



Figure 19a. Cratering Effects of Mt. Katmai Silicic Dust at Various Pressures with a Depth of 2.2 Inches



Figure 19b. Cratering Effects of Mt. Katmai Silicic Dust at Various Pressures with a Depth of 2.2 Inches

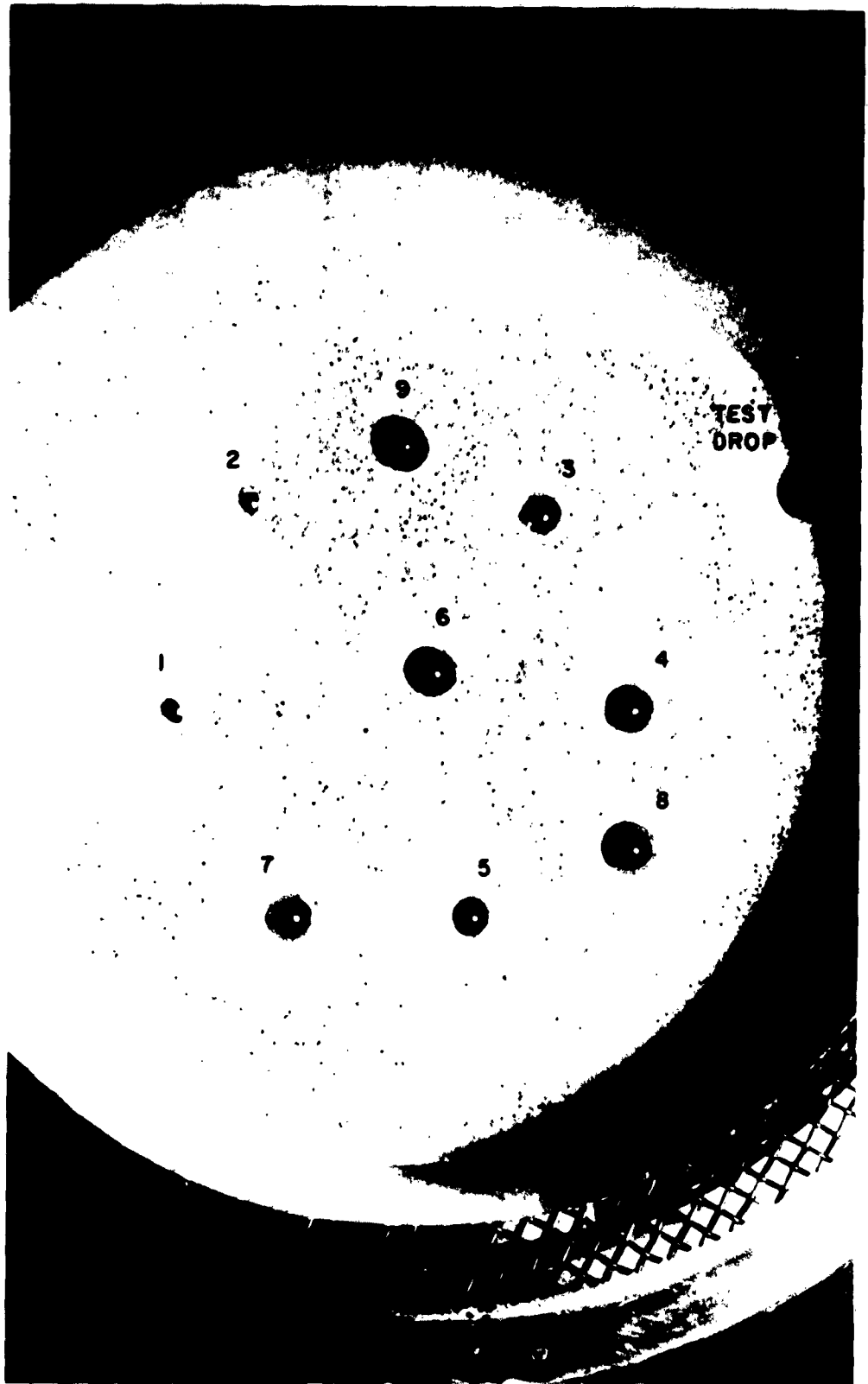


Figure 20. Cratering Effects of Ground Silicic Acidic Tuff Dust at Various Pressures with a Depth of 1 Inch

Hawaiian Phreatomagmatic

This natural volcanic basaltic dust was the subject of several control runs, as well as the final data run which produced the craters shown in Figure 17. This dust, like the Death Valley dust, was run at a depth of 2.2 inches. Figures 21, 24, and 27 show the results of the crater measurements. The data scatter is shown by the upper and lower limits of the vertical lines around the data point, and the uncertainty in pressure measurement is shown by the right and left limits of the horizontal lines about the point. In this and all subsequent runs, we used the drop pattern shown in Figure 15.

It will be noted from Figure 17 that the high-vacuum drops (balls 1 through 5) have irregular crater interiors, while the low-vacuum drops have smooth crater interiors. (The small dimples near craters 4 and 7 were caused by dust depth measurements) All impacts (except ball 3) were accompanied by a spray of fine dust.

3-F Pumice

The final data run of the finest dust tested is shown photographically in Figure 18. The crater measurements are shown graphically by Figures 22 and 25.

Although no data-scatter figures are available for the 3-F pumice, it should be noted that, by plotting a smooth curve consistent with the other test results, the data points were not deviated from appreciably.

Figure 18 shows (where the detail is not completely washed out) the usual pattern of the high-vacuum craters having irregular interiors, and the low-vacuum craters having smooth interiors. An exception is crater 5, which has a smooth interior (1×10^{-1} mm Hg) and crater 6, which has a rough interior (1 mm Hg). However, crater 6 was deeper than crater 5. The 3-F pumice and the Death Valley dusts produced craters quite similar in appearance.

Mt. Katmai Silicic

This Alaskan volcanic dust produced the most striking and unusual craters under impact. Photographs of the craters made in 2.2-inch dust are shown in Figures 19a and 19b.

Figures 21 and 24 show the measured impact parameters for the Mt. Katmai dust. Again, it should be apparent from the photographs why MDC measurements were not made. Although we allowed for no data scatter in plotting the curves, these curves agree quite well with the shape of the other curves except at low vacuum.

In craters 5 and 6 (Figs. 19a and 19b) some dust fell from the sides of the crater wall onto the top of the ball. Balls dropped at lower vacuum threw dust in large clumps for quite a distance. Some of this may be seen adhering to the cannister wall in both photographs. Ball 8 threw dust onto the inside of the bell jar up to 1 inch above the top of the cannister, and ball 9 threw dust 6 inches above the cannister.

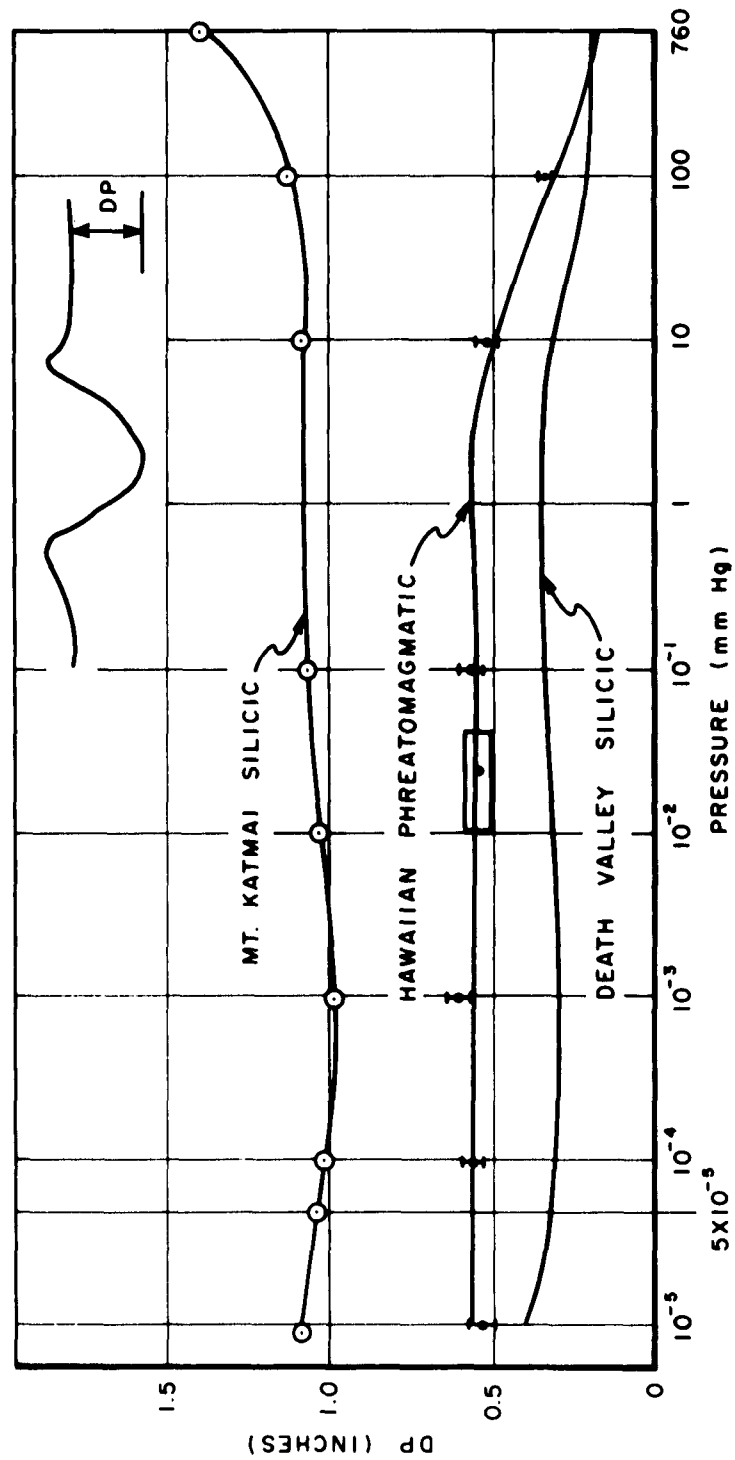


Figure 21. Depth of Penetration in Dusts 2.2 Inches Deep

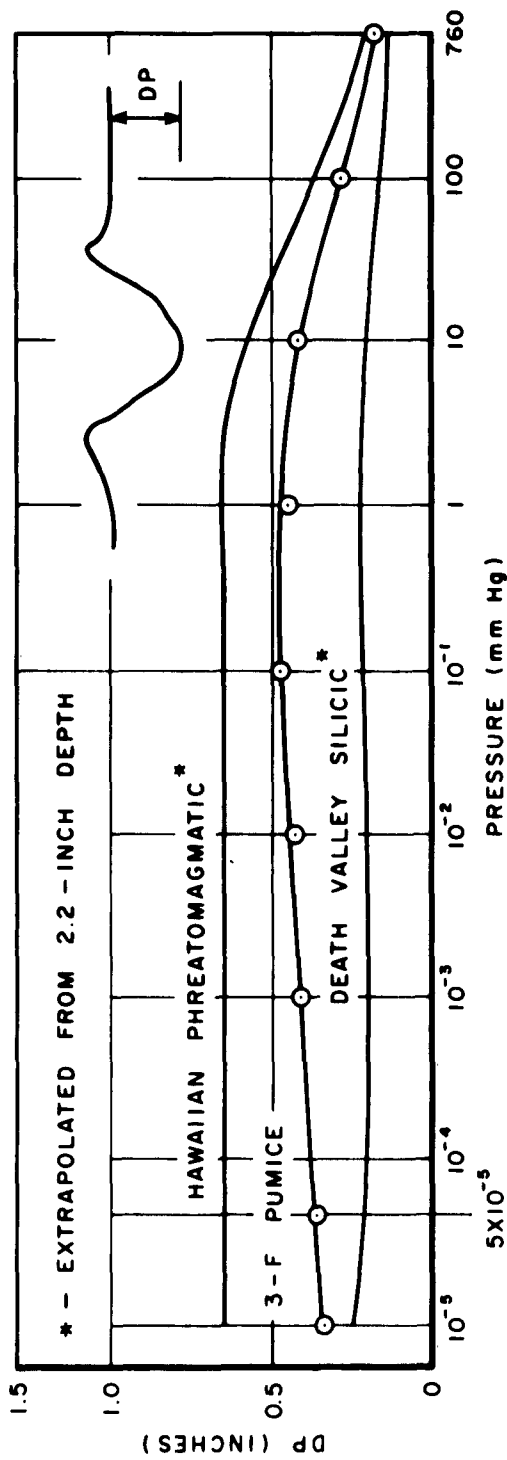


Figure 22. Depth of Penetration in Dusts 1.3 Inches Deep

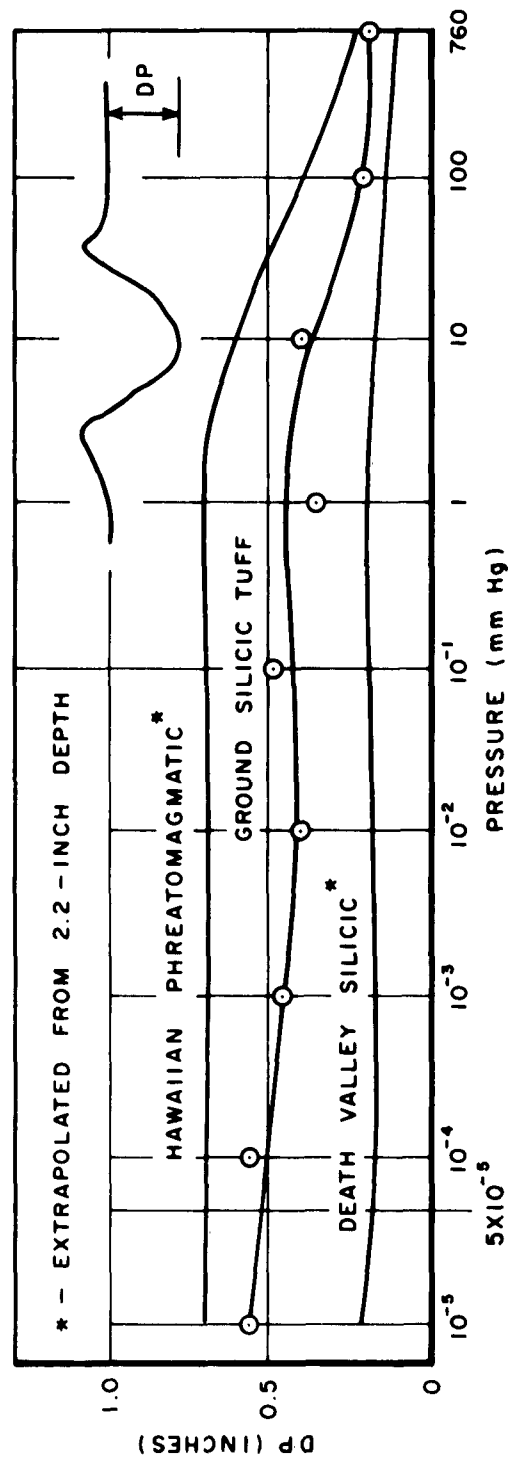


Figure 23. Depth of Penetration in Dusts 1.0 Inch Deep

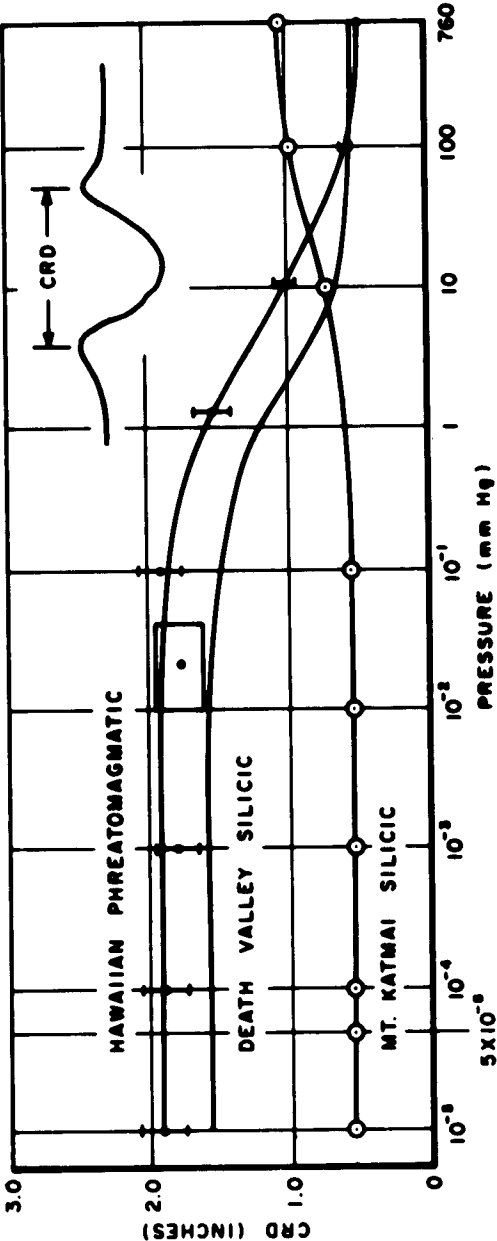


Figure 24. Crater Rim Diameter in Dust 2.2 Inches Deep

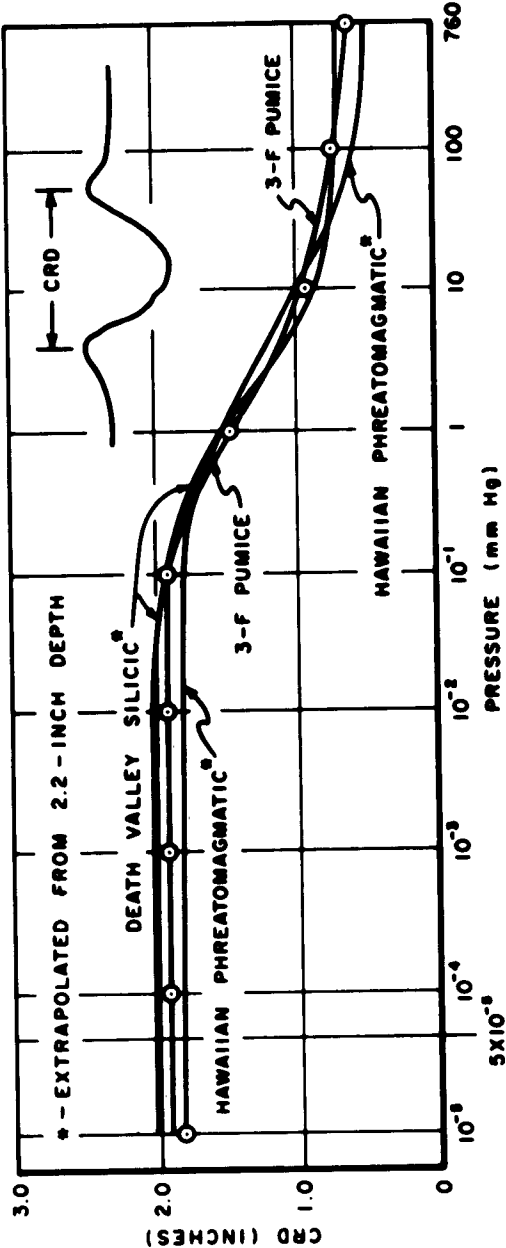


Figure 25. Crater Rim Diameter in Dust 1.3 Inches Deep

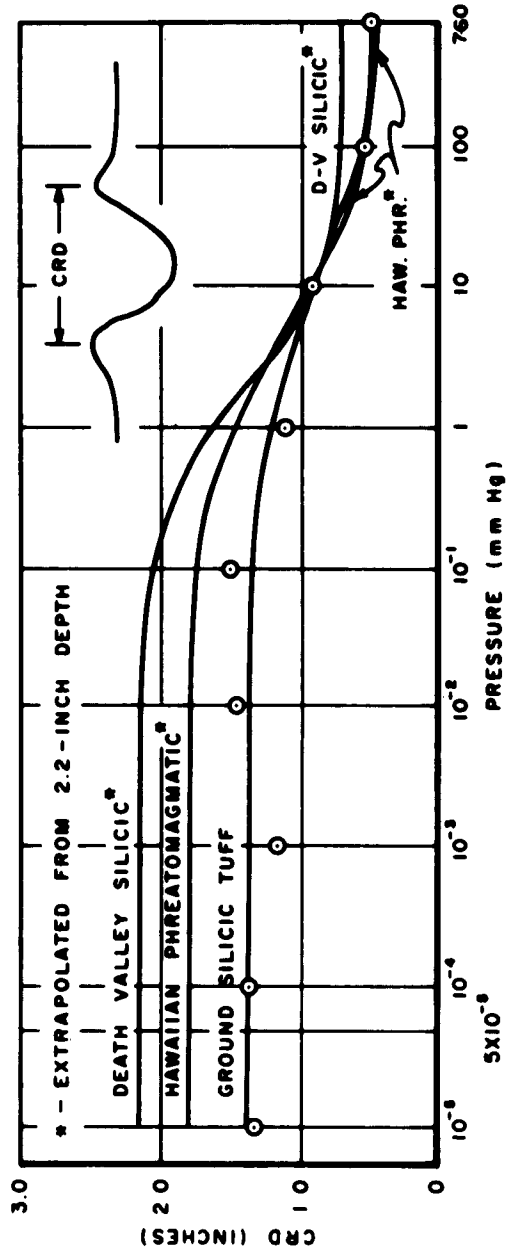


Figure 26. Crater Rim Diameter in Dust 1.0 Inch Deep

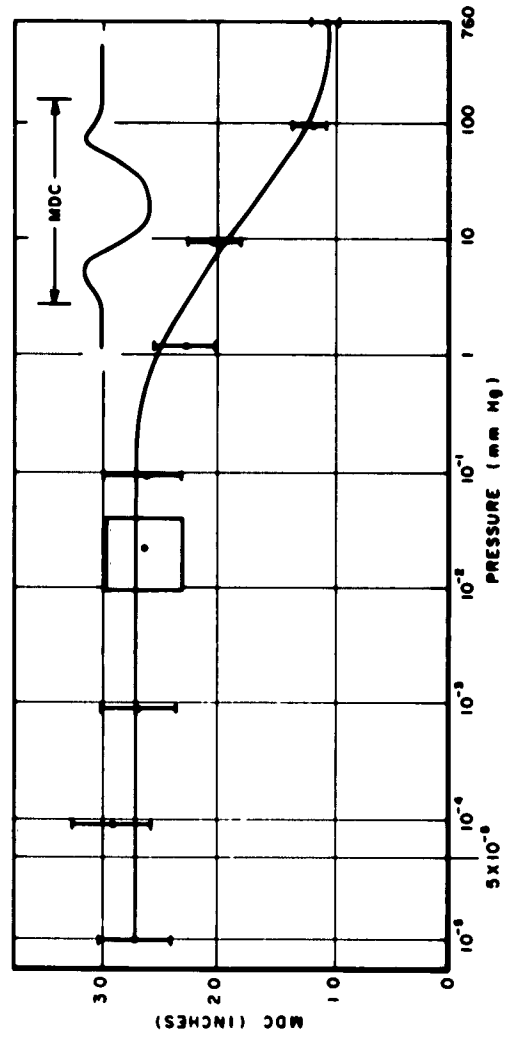


Figure 27. Maximum Diameter of Cratering in Hawaiian Phreatomagmatic Dust 2.2 Inches Deep

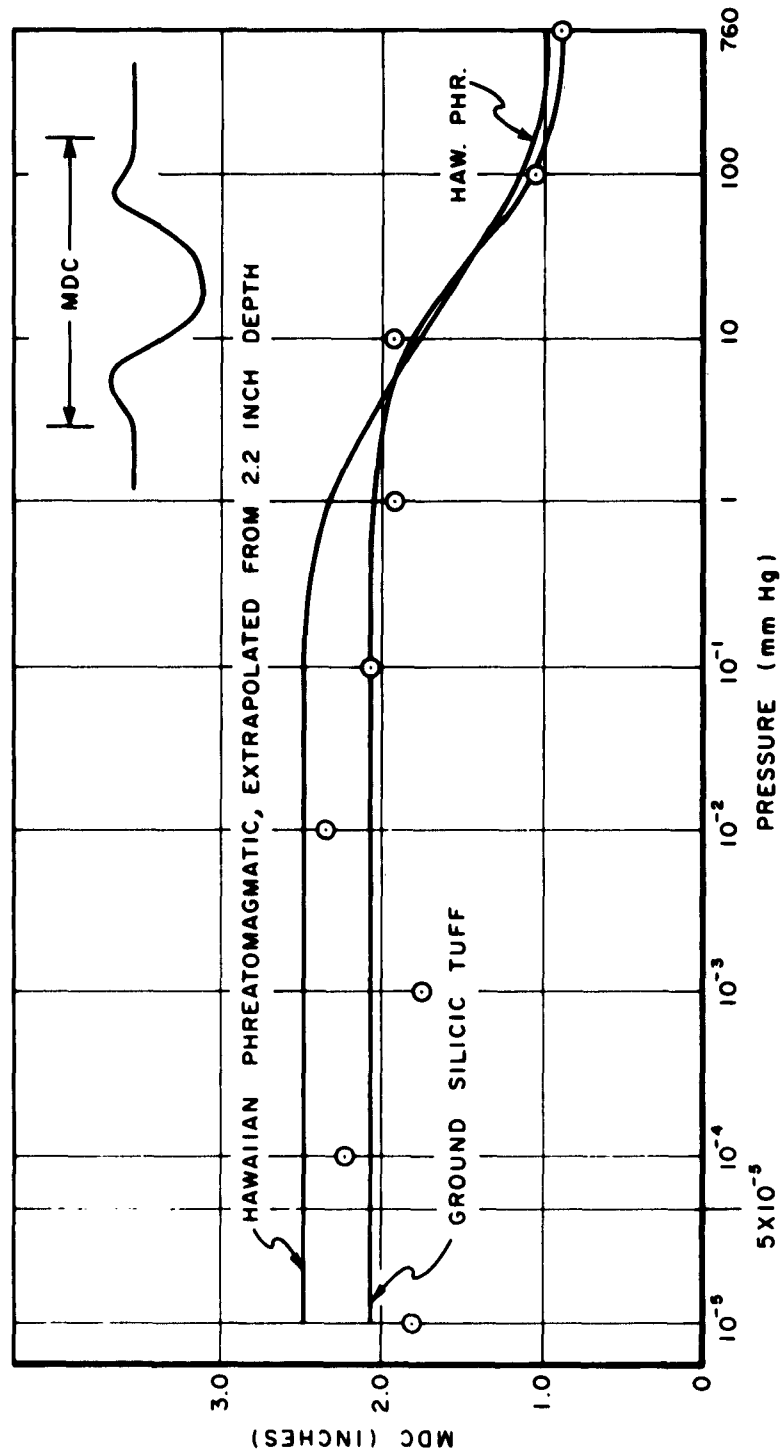


Figure 28. Maximum Diameter of Cratering in Ground Silicic Tuff Dust 1.0 Inch Deep

Ground Silicic Tuff

The artificially pulverized rock from California was not available in sufficient quantities to be run at depths greater than 1.0 inch. The craters produced by impact are shown in Figure 20 and graphs of the impact parameters are plotted in Figures 23, 26, and 28.

The scatter of data implied by Figure 28 is considerable and by Figures 23 and 26 is a little less. This data scatter is probably inherent in a run made at a shallow depth. In addition, the coarseness of the dust probably accounts for some data scatter. Drawing the curve through the observed points, which lie randomly on either side of the curve, would have assumed an unwarranted and inexplicable variation in impact parameters with vacuum. Since we cannot believe that the impact parameters vary in zig-zag fashion, it must follow that the data are highly scattered.

Figure 20 shows the nine balls that were dropped to gather data, plus a ball labeled "Test Drop" that was made as a preliminary check and not to gather data. All the craters were more or less circular with none of the dust clumps noted with the finer dusts. Drop 3, at 1×10^{-3} mm Hg, sent up a dense shower of dust in an instantaneous, stubby, fountain about 1 inch high and 1 inch out from the ball.

Hawaiian Composite Basaltic

The dust composed of pulverized basaltic pumice from Kilauea Volcano proved to be exceedingly difficult to measure. There was only enough dust to fill the 11-inch cannister to a depth of 0.8 inch. The balls dropped in this run, which was made in the standard manner, bounced out of their craters at pressures between 1×10^{-5} and 1×10^{-2} mm Hg. Because the bouncing balls tended to destroy the crater effects of both their own and previous drops, and because of general vagueness of crater outline, we decided to forego measuring the results on the grounds that the dust was insufficiently deep to permit accurate measurements.

The dust was tested again at a depth of 2.2 inches in a 4-inch cannister. Drops were made at 10^{-2} , 10^{-1} , and 1 mm Hg. The ball dropped at 10^{-2} bounced high, the ball dropped at 10^{-1} bounced slightly, and the ball dropped at 1 mm rolled out of its crater. Still another run was made later with 2.2 inches of dust in a 4-inch cannister. A single ball was dropped into the center of the cannister at 1×10^{-3} mm Hg. A series of single drops and measurements was then made with the 4-inch cannister at ambient pressure.

The crater made by the ball drop at 10^{-3} mm Hg in the Hawaiian composite was somewhat typical of the vacuum drops and will be described in detail. The crater consisted of three parts: a perfectly spherical depression left by the ball, an elliptical crater "blasted out" by the impact, and an elliptical area of out-throw immediately surrounding the crater where large and loosely packed dust particles had been thrown.

Because of the assorted conditions under which the data for the Hawaiian composite basaltic were obtained, the results have not been plotted but are tabulated in Table 4. Depth of penetration measurements proved impossible due to the bounce of the balls.

Italian Pumice

The Italian pumice was run at the same time the composite Hawaiian basaltic dust was run at 10^{-3} mm Hg. Because there was only enough pumice to fill a 4-inch-diameter glass bowl to a depth of 1.9 inches, measurements were made only at 10^{-3} and 760 mm Hg. Unfortunately, the dust was packed too loosely in the bowl and the results are very doubtful. The crater at 10^{-3} mm Hg was circular and very large. Some material was thrown 8.5 inches from the impact point. It is not known to what extent this was due to the looseness of the packing.

The results, such as they are, are shown in Table 4.

COMPARISON OF THE BEHAVIOR OF THE VARIOUS DUSTS

Figures 21 through 28 and Table 4 give comparisons between the various dusts. Because of the necessity of using various depths of dust, direct comparisons between all seven dusts tested cannot be made. As was explained earlier, the measured curves from the tests run on the Death Valley silicic and Hawaiian phreatomagmatic dusts at 2.2 inches have been roughly corrected to other depths to provide a basis of comparison.

Although the comparison of the various dusts is presented graphically (Figs. 21 through 28), tabularly (Table 4), and photographically (Figs. 16 through 20), a summary is also included in Table 5 for convenience.

TABLE 4
COMPARISON OF PARAMETERS AT VARIOUS PRESSURES

A. DUST DEPTH OF 2.2 INCHES						
Pressure mm Hg	Ground Hawaiian Composite Basaltic		Death Valley Silicic		Hawaiian Phreatomagmatic	
	CRD	MDC	CRD		CRD	MDC
.001	1.21	1.43	1.58		1.93	2.69
.01	0.7	0.7	1.58		1.91	2.69
.1	1.11	1.11	1.5		1.86	2.69
1.0	1.3	1.3	1.2		1.6	2.52
760	1.06	1.06	.54		.48	1.05
B. DUST DEPTH OF 1.9 INCHES						
Parameter	Italian Pumice		D-V Silicic*		Hawaiian Phreatomagmatic	
	0.001	Sea Level	0.001	Sea Level	0.001	Sea Level
DP	0.652	0.386	0.267	0.178	0.596	0.201
CRD	2.17	0.73** 0.57***	1.73	0.59	1.89	0.47
MDC	2.82	1.8** 0.57***			2.63	1.03
* Corrected from 2.2-inch depth ** Loosely packed *** Tightly packed						

TABLE 5
DUST COMPARISON SUMMARY

Particle size distribution (in order of increasing coarseness):
3-F pumice Death Valley silicic Mt. Katmai silicic Hawaiian phreatomagmatic basaltic Ground acidic silicic tuff Ground Italian pumice Ground Hawaiian composite basaltic

Depth of Penetration (in order of increasing penetration):

At high vacuums	At low vacuums	At sea level
D-V silicic 3-F pumice Ground tuff Hawaiian phr. Mt. Katmai	D-V silicic Ground tuff 3-F pumice Hawaiian phr. Mt. Katmai	D-V silicic* 3-F pumice Ground tuff Hawaiian phr.* Mt. Katmai

Crater Rim Diameter (in order of increasing diameter)

At 2.2-inch depth:

At high vacuums	At low vacuums	At sea level
Mt. Katmai D-V silicic Hawaiian phr.	D-V silicic Mt. Katmai Hawaiian phr.	Hawaiian phr. D-V silicic Mt. Katmai

At 1.3- to 1.0-inch depth:

At high vacuums	At low vacuums	At sea level
Ground Hawaiian composite, and Ground tuff Hawaiian phr. 3-F pumice	D-V silicic 3-F pumice and Ground tuff	Hawaiian phr. Ground tuff 3-F pumice D-V silicic, and Italian pumice Ground Haw. comp.

Maximum Diameter of Cratering (in order of increasing diameter):

At 1.3 to 1.0 inches:

At high vacuums	At low vacuums	At sea level
Ground Haw. comp. Ground tuff Hawaiian phr.	Ground Haw. comp. Ground tuff, and Hawaiian phr.	Italian pumice Ground tuff Hawaiian phr. Ground Haw. comp.

* At less than 2.2-inch depth. These positions reverse at 2.2 inches.

POSSIBLE EXPLANATIONS OF VARIATIONS IN IMPACT BEHAVIOR AT VACUUM

Any attempt to set forth a single hypothesis to explain the behavior of these lunar dust models would not only be presuming more knowledge of molecular phenomena than the author possesses, it would also be inadequate to explain all the observed facts. Inasmuch as the depth of penetration curves show two inflection points (the Hawaiian phreatomagmatic only shows one), it is likely that two processes, at least, are operative here.

In the first stages of air removal, the presence of air between the dust particles probably provides a cushion to absorb the impact forces. Thus, as this air is removed, the dust particles can travel further under the impulse given by the ball and produce deeper penetrations and wider craters.

At around 1 mm Hg (for depth of penetration) to 10^{-2} mm Hg (for crater rim diameter) the air is completely removed, insofar as this effect is concerned. Now the effect of the adsorbed molecules on the dust surfaces becomes the factor governing the dynamic behavior of the dust. Although there is little effect on the width of the crater, the effect of removing more and more layers of adsorbed molecules is noticeable in changing the depth of penetration.

Successive reduction in the adsorbed layer of molecules probably has two effects: An increase in the cohesive forces between the particles, and a change (probably, but not necessarily, an increase) in the coefficient of friction among the particles.

That the force between molecules increases with decreasing distance has long been known and has been measured for microscopic bodies (Ref. 10). Since the dust is vibrated under vacuum, the particles may come closer together as the adsorbed gas layers are stripped off. This force may be partially responsible for the dust clumping at high vacuums. That the adsorbed layers of gas play a part in friction cannot be disputed (see Appendix E and Ref. 30). However, the effects of high vacuum on inter-particle friction in a dust have never been theoretically investigated.

Yet another possible cause of the effects observed is electrostatic. Agitation of small particles in vacuo may produce a static charge (Ref. 8:26). Certainly the variation in electrostatic charge could affect the dust particle dynamics.

Unfortunately, this discussion of possible explanations for the behavior of the dust particles does not include the Mt. Katmai silicic dust. At high vacuum, the curves for the Mt. Katmai dust show the same general slope and inflection points as for the other dusts, albeit with greatly different values; hence, the behavior may be explained in the same terms. Apparently the air-cushion hypothesis has little or no relevancy for the Mt. Katmai dust. Clearly, the clue to the anomalous behavior of this dust lies in its microstructure.

Although tentative explanations are possible, an exact explanation of the observed behavior of the various dusts must await a more detailed study.

MEANING OF THE RESULTS FOR LUNAR ENVIRONMENTAL SIMULATION

The curves of Figures 21 through 28 show that the CRD and MDC values for all the dusts do not vary significantly at pressures past 10^{-2} mm Hg, but the DP values change continuously up to 10^{-5} mm Hg (with the exception of the Hawaiian phreatomagmatic dust). Therefore, any lunar environmental simulator must provide vacuums higher than 10^{-5} mm Hg to completely simulate whatever conditions actually exist on the lunar surface. Equally important, no single dust should be chosen as the lunar dust model. A simulator must provide a variety of dust "floors" for the testing of equipment.

The operation of the high-vacuum bell jar with finely divided dust samples was feasible, although several problems occurred, chiefly "fountaining" of the dust during fast pump-down at approximately 1 mm Hg. There is no theoretical or practical reason to believe that large quantities of dust cannot be handled effectively in a lunar simulation chamber.

SECTION 5

CONCLUSIONS

SUMMARY

An analysis of the factors relevant to lunar environmental simulation showed that the behavior of lunar dust models in various vacuums must be studied to help establish the degree of vacuum required of a lunar simulator. The reasons for selecting various silicic and basaltic rock dusts as lunar dust models have been discussed and the origin, particle size distribution, and microstructure of the dusts have been examined.

A review of the test procedure has been given. The effect of hold time, walls of the container, dust depth, local density irregularities, and composition of the residual gases have been examined and shown to be important in interpreting the data. Although crater width measurements indicate dusts do not change their behavior at pressures lower than 1×10^{-3} mm Hg, depth of penetration measurements continue to change at pressures less than 1×10^{-5} mm Hg.

No single test at a single level of pressure can predict the entire behavior of a dust at other levels of pressure. The behavior of a dust is a function of not only its particle size distribution, but also of its microstructure.

The conclusions may be summarized in three main points:

1. Many variables must be considered in comparing the behavior of lunar dust models in a vacuum. Any comparison of dusts at a single vacuum, by a single measurement, or at a single (especially a shallow) depth is of little value.
2. In analyzing the behavior of a dust in vacuum, we must consider the kinds of gases present, the particle size distribution, and the microstructure of the dust.
3. The width of a standard impact crater in the lunar dust models tested does not vary at pressures lower than 10^{-3} mm Hg. The depth to which a ball will penetrate the dust when dropped from a standard height does change continuously for most dust models at pressures lower than 10^{-5} mm Hg.

RECOMMENDATIONS

The main purpose of this study was to determine the limit (or lack of limit) beyond which the dynamic behavior of a lunar dust model does not change. Inasmuch as we determined that no limit exists at vacuums as high as 10^{-5} mm Hg, this study should be continued at higher vacuums. Lunar simulation will require vacuums of at least 10^{-5} mm Hg, but how much more is still unanswered.

The various dusts used in the test were discussed, and the dusts used by other experimenters were mentioned. The number of dust samples should be increased to include at least the olivine basalt used by NASA.* Basaltic dust from other sources than Mt. Kilauea

* Letter from Dr. L. D. Jaffe, Chief, Materials Research Section, Jet Propulsion Laboratory (NASA), Pasadena, California (23 May 1961).

should be tested, and some of the dusts should be tested again in larger quantities. (Other workers in this field might run tests on the samples used in this investigation to correlate the results with values obtained in this study.)

A detailed analysis of the test methods was presented. From this analysis it should be apparent that many uncertainties exist in the basic technique. The effect of all the variables, but especially hold time, dust packing density, and dust shallowness should be examined in greater detail for each dust tested to produce a truly valid study with a minimum of uncertainty. Each run should be made several times to validate the experimental points.

This study could only be preliminary to a more intensive study using the same methods. In addition, this study should also be made the basis of another type of study in which the shear strength and penetration resistance of lunar soil models are examined under vacuum conditions using standardized techniques. Results of this study would be of immense value to the designers of lunar vehicles.* (See Ref. 19 in toto as background.)

Finally, it is recommended that the designer of lunar vehicles consider the clumping effect of fine dust particles in vacuo and be prepared for a lunar dust that may support a greater or a lesser load than the same dust in an atmosphere.

* Letters from Capt. R. A. Liston, USA, Chief, U. S. Army Land Locomotion Laboratory, Detroit, Michigan (20 January and 13 March 1961).

Also telephone conversation (1 May 1961) and letter (21 June 1961) from Messers. J. H. Halajian and R. Stewart, project engineers, Grumman Aircraft Engineering Corporation, Bethpage, New York.

Also interview with Mr. R. Immonen, project engineer, Bendix Systems Division, Bendix Corporation, Ann Arbor, Michigan (23 June 1961).

APPENDIX A

A SURVEY OF LUNAR SURFACE CONDITIONS

To provide a background for this thesis, the more significant features of the lunar environment should be considered in more detail. A glossary of the various astronomical and geological terms used in this discussion will be found in Appendix G.

A great deal is known about the moon. Indeed, basic astronomical information is known to considerable accuracy. The moon is some 2170 miles in diameter and its surface area is about 0.074 that of the earth. The surface gravity is 0.164 that of the earth, which requires an escape velocity of 1.5 miles/sec. Its day (period of rotation with respect to the sun) is equivalent to 27.322 earth-days.

The lunar surface is characterized by maria, or large dark areas, that are generally thought to be lava flows (Refs. 17:64, 16:11). These maria are divided by lighter-colored areas of high steep mountains and large craters. The smallest observable crater on the moon is 500 feet in diameter (Ref. 28:2) and the largest is 183 miles in diameter (Ref. 1). The mountains rise to heights of up to 33,000 feet above the valley floors (Ref. 28:2).

The temperatures measured on the lunar surface generally agree well. It must be remembered, however, that temperature measurements made on the moon are not equivalent to temperature measurements made on planets with an appreciable atmosphere. A thermocouple measuring radiation from a portion of the lunar dish will give an average of all exposed and shadowed surfaces. Consequently, subsolar temperatures are relatively high, and temperatures of areas near the terminator (the line between lunar night and day) are relatively low. However, areas exposed to the sun at the terminator will receive exactly as much sunlight as they would at the subsolar point. Since nearly 180 spherical degrees of radiative heat-sink at 5°K are available to both terminator and subsolar objects, the temperatures attained will not be too dissimilar.

Another factor of interest in considering the thermal environment of the moon is the 2°40' polar zone (one lunar degree is about 18.85 miles) available for a six-month polar night or day cycle (Ref. 15).

The subsolar point can have a temperature as high as 374°K (Ref. 18:7). The temperature drops to below 250°K at the terminator (Ref. 18:8). The temperature drops to a minimum value of 120±5°K on the dark side of the moon within a few earth-days of sunset (Ref. 18:9-11). The effect of earthshine on the moon is negligible (Ref. 18:20).

The size, mass, astronomical motions, gross physical appearance, and surface temperatures are the surface features of the moon which can be measured optically. These features of the lunar environment are all generally agreed upon.

Some features to be discussed subsequently are not only not agreed upon as to existence or origin, they are the subject of great controversy. This appendix is not meant to sway the reader to one side or another of the controversies. It is intended only to point out that different concepts exist and, in general, what these concepts are.

The chief controversy concerns the origin of the craters, or "ring-walls," of the moon. Some believe these craters to be caused by meteorites and others believe they are volcanic calderas (not volcanic eruptions). Perhaps the best arguments for the meteoric

hypothesis are given by Urey (Ref. 31) and Baldwin (Ref. 4). The volcanic hypothesis is well defended by Green (Ref. 16), Moore (Ref. 22), and Firsoff (Ref. 15).

Green points out the difference the two hypotheses would make to the construction of a picture of the lunar surface. If the surface resulted from a heavy meteoric in-fall, one would expect considerable rock flour and stony, stony-iron, and iron-nickel meteoric fragments. Considerable rubble would be created by the enormous impact energies and some odd matrices of meteorite fragments would be imbedded in pulverized and fused silicates (Ref. 16:11).

Although the general theories of meteoric impact are well understood, the concept of the volcanic processes that might have formed the lunar features is less well known.* Essentially, the concept is this: A flow of magma builds up pressure under an existing volcano or dome of overlying rock. The molten rock subsides more-or-less suddenly after producing a general swelling of the overlying rock. The overlying rock, deprived of its support, collapses suddenly, with or without an explosion, to form a caldera. A secondary volcanic cone is often produced in a more-or-less central location in the caldera. An example of this process is the caldera of collapse known as Crater Lake in Oregon.

The craters of the moon often have central peaks with summit craters. They are located along well-defined lines and in certain areas rather than being randomly distributed. And no older crater is ever smaller than a younger crater, indicating an invariant decrease in the activity of the causative agent.

That the lunar surface is dust-covered no one is prone to argue. The measurements of Piddington and Minnett (Ref. 25:281-282, 284) proved this beyond any reasonable doubt. The dust layer has been confirmed by other microwave measurements, radar measurements (Ref. 7:408), and light reflection and polarization measurements (Ref. 13:57). The estimated thickness and composition vary, however. Pawsey and Bracewell believe the model of Jaeger and Harper to be the best (Ref. 25:282). This model provides for a 0.1-cm-thick dust layer of unspecified composition overlaying a pumice-like layer of undetermined thickness. Piddington and Minnett believe the average thickness of the lunar dust to be 40 cm (Ref. 26:63). Urey feels that a very acidic granitic-type rock is prevalent at the surface (Ref. 31:1680). Firsoff feels that the area near the crater Aristarchus may be covered with sulfur (Ref. 14:164), but that pumice is to be expected elsewhere. Kulander believes the lunar dust is "at least 10 cm deep and probably considerably deeper" over the entire lunar surface (Ref. 18:46). Green gives dust thickness limits of 0.001 to 1 meter for the maria and 1 to 1000 (!) meters for the nonmaria areas.

There is general agreement (Ref. 18:46) that the cosmic in-fall of dust must be quite meager.** This in-fall consists of iron-nickel spherules, such as may be found on the floors of our oceans (Ref. 9), and micrometeorites. Were this in-fall appreciable, we would see no color contrast on the moon.

* Particularly by those that criticize the volcanic theory. See, especially, Ref. 7:64, 68.

** This was also confirmed by an interview with Dr. J. Green, Aero-Space Laboratories, North American Aviation, Downey, Calif. (23 March 1961).

Lunar dust may also be formed by thermal shock cycling, which would tend to cause the following: exfoliation of the exposed rocks; ionic bombardment (with unknown effects); meteoric impact, which would cause rock flour; and volcanic processes, which could cause dusts of assorted sizes, types, and quantities (Ref. 2:3).

The amount and composition of the lunar atmosphere is yet another subject of dispute. Perhaps the highest estimate seriously given for the density of the lunar atmosphere is 0.0001 that of the atmosphere at the earth's surface (Ref. 15:130). More pessimistic calculations have placed the value at 2×10^{-13} that at the earth's surface (Refs. 6:1606, 12:1040-6). This last estimate is about the ultimate in pessimism, in that it corresponds to the particle density believed to exist in cislunar space and means, in effect, that no lunar atmosphere whatsoever exists. It is difficult to refute any estimate of the lunar atmosphere made within these limits, because they correspond roughly to the uncertainty in our observations, unless the experiments of Dollfus in 1952 and Costain, et al., in 1956 be accepted as valid. Apparently not all selenologists accept their data. Dollfus established an upper limit of 2×10^{-6} that of the earth's atmosphere, or 1.52×10^{-3} mm Hg, and Costain, et al., reduced this to 2×10^{-10} earth's atmosphere, or 1.52×10^{-7} mm Hg (Ref. 6:1606). Most conservative workers believe that 1×10^{-6} mm Hg is an acceptable upper limit to the lunar atmosphere (Ref. 16:12). The variation between whatever limits are established by observation is dictated by the basic assumptions concerning the origins of the lunar atmosphere.

One of the most strongly entrenched beliefs about the moon holds that it is a dead world and has been so for eons. This school of thought denies the moon any current or recent volcanic processes that would evolve gas. This group is composed primarily of theoreticians.

Another group, composed primarily of observers, feels that volcanic processes are still operative on the moon. They point to the gas eruption from the central peak of Alphonsus in November 1958, and the spectrograms of C_2 and C_3 obtained by N. A. Kozyrev of the Crimean Astrophysical Observatory (Refs. 15:56, 28:2, 17:64, 65).^{*} Other evidence of vulcanism includes the disappearance of the Linne' crater. A crater 6 miles wide and 1000 feet deep disappeared several decades ago and was replaced by an insignificant craterlet surrounded by a white halo (Ref. 15:140). Certain craters (Gaimaldi and Endymion) show regular changes during lunation, and Plato shows an irregular variation apparently due to local mists on the crater floor (Ref. 15:140). (See also Ref. 22.)

The low escape velocity still permits the moon to retain water vapor (possibly), carbon dioxide (Refs. 15:135, 136; 16:12), argon, xenon, krypton, and other heavy gases (Refs. 15:135, 136; 16:12, 28:3). In examining the gas analysis from a typical volcano (Table 6), we find that the moon could be expected to retain all the volcanic gases except hydrogen, nitrogen, and possibly water vapor.

^{*} The "dead-world" school does not deny Kozyrev's observation, but states that he saw trapped gas escaping, rather than volcanic activity (Ref. 17:64, 65). That the evolution of trapped gas cannot create a lunar atmosphere can only be explained in terms of evolution being a very rare event in geologic time. One may also inquire as to how a gas is released from its "trap" on a world where nothing changes.

TABLE 6
ANALYSIS OF GASES FROM KILAUEA VOLCANO 1917-1919

Gas	Weight %
H ₂ O	45.12
CO ₂	20.71
CO	0.67
H ₂	0.06
N ₂	7.93
A	0.3
SO ₂	16.67
SO ₃	5.51
S ₂	2.47
Cl ₂	0.54 (from Ref. 33:239)

It is interesting to note that gases obtained by heating igneous rocks in vacuo have a similar composition (Ref. 33:239).

As mentioned previously, there is probably a very small amount of hydrogen present in the lunar atmosphere, originating not from volcanic processes, but rather from sweep-out of the hydrogen present in cislunar space and from solar proton and electron bombardment. This gas would reach some equilibrium concentration and would constitute a greater or lesser portion of the lunar atmosphere, depending on the amount of volcanic gases exhaled and retained.

Other significant features of the lunar environment include particulate radiation, magnetic field, and meteorite bombardment. Not much is known, or even speculated, about these factors. The particulate radiation is believed to be variable, possibly with heavy primary cosmic rays and dangerous periods of radiation during solar-flare activity. The magnetic field is probably no more than 0.05 that of the earth (Ref. 28:3). Meteoric bombardment is probably no more dangerous on the moon than in cislunar space -- that is, the danger is unknown but probably fairly small.

APPENDIX B

REDUCED GRAVITY SIMULATION IN A LUNAR ENVIRONMENTAL SIMULATOR

In order to simulate the effect of a reduced gravity, the actual effect of gravity on the object under test must be considered. If we are testing the traction of a tracked vehicle, the simplest and most effective way to simulate the reduced gravity is to reduce the mass of the tractor by removing nonessential components, and ballasting for proper weight, center of gravity, and moments of inertia. If the floor of the simulator has been made a realistic model of the moon's surface by a covering of a well-chosen series of dusts and rocks, and the vacuum is sufficiently high, the traction test should be as faithful as can be had.

Other types of tests will require other, but basically similar, approaches. Suppose it is desired to investigate the behavior of the lunar dust layer under the jet of a rocket making a tail-first touchdown. In this case, dust particles are given an impulse that moves them through an atmosphere of sharply varying properties as it thins into a vacuum a few feet from the exhaust.

To have the dust particles in the simulator behave as dust particles on the lunar surface do, three dimensionless ratios must be the same for the test situation as for the real situation: Mach number, Reynolds number, and Froude number.

The Mach number is defined as the inertia force divided by the elastic force, or the ratio of the velocity of the gas divided by the local speed of sound. Attaining the proper Mach number in a test nozzle is not a function of the lunar simulator chamber itself. It will not be discussed, therefore, beyond the observation that the chamber must have a pumping rate sufficient to carry off the exhaust gases as fast as they are generated.

The Reynolds number is defined as the inertia force divided by the viscous force, or the ratio of the product of the gas density, speed, and the dust-particle diameter divided by the viscosity of the gases.

$$NR = \frac{\rho v \ell}{\mu} \quad (1)$$

This ratio may be satisfied by using the same combustion gases in the same ratio in the model as in the actual item, and by using the same particle size as we would expect with a lunar dust.

The Froude number is defined as the inertia force divided by the gravity force:

$$NF = \sqrt{\frac{v^2}{\ell g}} \quad (2)$$

where:

- V = the speed of the gas,
- ℓ = the particle diameter, and
- g = the local acceleration of gravity.

To achieve the proper NF, the following relationship (from Ref. 27:264) must be satisfied:

$$W_m = W_{fs} \frac{\rho_m}{\rho_{fs}} \left(\frac{l_m}{l_{fs}} \right)^3 \quad (3)$$

where:

W_m = the weight of the model dust particle,

W_{fs} = the weight of full scale (lunar) dust particle,

ρ_m = the density of gas used in the simulator,

ρ_{fs} = the density of the gas used on the moon,

l_m = the diameter of the simulated dust particle, and

l_{fs} = the diameter of the actual lunar particle.

Assuming:

$$\frac{\rho_m}{\rho_{fs}} = 1 \quad \text{and} \quad \frac{l_m}{l_{fs}} = 1,$$

then:

$$W_m = W_{fs} \quad (4)$$

for simulation.

Or,

$$M_m \left(\frac{g_e}{g_c} \right) = M_{fs} \left(\frac{g_{fs}}{g_c} \right) \quad (5)$$

where:

g_e = the earth's gravitational acceleration,

g_{fs} = the moon's gravitational acceleration,

g_c = the conversion factor from weight to mass units,

M_m = the mass of the model dust particle, and

M_{fs} = the mass of the actual lunar dust particle.

Since:

$$g_e = 6 g_{fs} \quad (6)$$

$$M_m = \frac{M_{fs}}{6} \quad (7)$$

Thus, we must have a dust particle of the same size but one-sixth the mass for proper dynamic simulation.

No attempt has been made to actually select or test suitable materials for the dynamic simulation of lunar dust at reduced gravity, but some random density figures might be of interest. Basaltic lava can have a density of 180 pounds per cubic foot. To simulate dust of this density, dust of 30 pounds per cubic foot density would be required. Certain pumices might meet this value in the larger particle sizes, and possibly charcoal, dry gypsum, and certain types of sawdust. Whether the behavior of these particles with respect to each other would resemble that of lunar soils in a vacuum is another matter entirely.

Another point that should be discussed here is the question of dust compaction under reduced gravity. For a dust depth of 1 inch or so, there is probably not a great deal of difference, but compaction at greater depths is a matter of speculation. If moonquakes are frequent and strong enough, the dust will probably compact itself without much reference to the weight of the dust above, except in depths of over a foot or so. If the only force packing the dust is the overlying weight, that force will be very significant. Perhaps the only thing that can be said definitely here is this: When dealing with simulator dusts that are not density reduced, special care should be taken to leave them relatively loosely packed.

A discussion of reduced gravity simulation would not be complete without mentioning the work of the Aero-Space Laboratories of North American Aviation (Ref. 2:10-22) where gas-injection model studies have been carried out on lunar dust models with a consideration of the reduced gravity effects. Mention should also be made of the Lewis Research Center studies on gas injection onto dust surfaces at vacuum, although this study was not as complete.*

* Letter from Mr. L. J. Obery, Chief, Propulsion Aerodynamics Branch, Rocket and Aerodynamics Division, Lewis Research Center, NASA, Cleveland, Ohio (14 June 1961).

APPENDIX C

A PARTIAL SURVEY OF PRESENT SPACE SIMULATOR FACILITIES
RELEVANT TO THE DESIGN OF A LUNAR ENVIRONMENTAL SIMULATOR

A study of lunar environmental simulation would be incomplete without a survey of those facilities relevant to the design of a lunar simulator. No hard-and-fast rule was made to define this relevancy, and certain facilities were included or excluded from this list for admittedly arbitrary reasons. We do not claim that this list is complete, but it probably represents the majority of appropriate facilities.

Ideally, a lunar environmental chamber should be large enough to not only contain both present and future lunar-bound equipment, but provide room for whatever maneuvers are necessary. It should have a very large continuous evacuation capability and should be capable of high vacuum. It should have provisions for simulation of thermal radiative environment. The following is a partial listing of present, future, and proposed facilities of interest to the designer of a lunar simulator.

AERONAUTICAL SYSTEMS DIVISION

An 8 by 25 foot (horizontal) vacuum chamber capable of 10^{-7} mm Hg is in operation at Wright-Patterson Air Force Base. This chamber is used by the Space Propulsion Section of the Propulsion Division, ASD. The chamber has a liquid nitrogen cold trap but no source of radiant heat or cooling. A liquid hydrogen cryowall is being installed, however.

BENDIX SPACE SYSTEMS DIVISION

The Bendix Corporation, Ann Arbor, Michigan, has two facilities of interest. One chamber, 4 by 8 feet, is capable of vacuums of 4×10^{-9} mm Hg in the clean, empty configuration. Solar simulation is by a carbon arc projection lamp. The temperature may be controlled between -400°F and $+2000^{\circ}\text{F}$. The radiant heat sink consists of liquid nitrogen baffles. A liquid nitrogen cold trap is used.*

The other Bendix facility of interest is a chamber 20 by 27 feet capable of vacuums of 5×10^{-7} mm Hg. This chamber is scheduled for completion 1 December 1961. Pumping rates are 150,000 liters/sec at 1×10^{-3} mm Hg, 180,000 liters/sec at 2×10^{-4} mm Hg, 168,000 liters/sec at 1×10^{-6} mm Hg. Solar simulation is by carbon arc lamp projection.*

GRUMMAN AIRCRAFT ENGINEERING CORPORATION

Grumman has a vacuum chamber measuring 48 by 100 inches capable of vacuums to 10^{-8} mm Hg. They are presently running shear and penetration tests on four types of soil under vacuum in this chamber.**

* Letter from R. C. Klein, project engineer, Environmental Laboratory, Bendix Space Systems Division, Ann Arbor, Michigan (26 June 1961).

** Telephone conversation 1 May 1961 and letter 21 June 1961 from J. Halajian and R. J. Stewart, project engineers, Grumman Aircraft Engineering Corp., Bethpage, N. Y.

LITTON INDUSTRIES

Litton Industries, Space Research Laboratory, of Beverly Hills, California, has proposed to the National Aeronautics and Space Administration the construction of a "National Lunar Laboratory." In order not to disclose proprietary information, it will suffice to say the proposed laboratory is a large lunar environmental simulator and the proposal (Ref. 31) would be of extreme interest to a designer of such simulators.

Litton has an 8 by 15 foot (horizontal) chamber capable of 10^{-6} mm Hg. Pumping is by diffusion pumps and cold traps. Liquid nitrogen baffles are used as heat sinks. Radiant-heat sources are external to the chamber. An interesting feature of this chamber is its habitability; that is, it has been operated at vacuum with a worker inside (Ref. 31).

SPACE TECHNOLOGY LABORATORIES

The space-thermal-environment-simulation facility of Space Technology Laboratories, Los Angeles, California, is 12 feet long and 7 feet in diameter. The space environment is claimed to be duplicated to within 10 percent. The rays from a solar simulator are beamed into the chamber through a 10-inch port. Liquid nitrogen baffles are used as a radiative heat sink. A vacuum of 9×10^{-7} mm Hg is obtainable with a clean empty chamber. The pumping system is composed of a 4000-liter/sec oil-vapor diffusion pump and a 130-cfm mechanical roughing pump. The chamber may be heated to 200°F and cooled to -20°F (Ref. 27).

U. S. ARMY

The Engineer Research and Development Laboratories, Fort Belvoir, Virginia, has proposed a facility that is 10 meters in diameter with an inside work space that is 8 meters in diameter and 5 to 9 meters high. They propose a vacuum of 10^{-6} mm Hg and a liquid nitrogen heat sink.*

VOUGHT ASTRONAUTICS

The Vought Astronautics hyper-environment space simulator is a 10 by 10 foot cylinder with a vacuum capability of 1×10^{-7} mm Hg. The pumping speed for a 1×10^{-6} mm Hg vacuum is 36,000 liters/sec. The solar spectrum is simulated by a single mercury xenon lamp, which matches the solar spectrum well except for near infrared. The radiant heat sink is a liquid nitrogen shroud with a flow rate of 8250 lbs/hr, which produces inner wall temperatures between 77 and 100°K (Ref. 30).

* Letter from H. N. Lowe, Deputy Chief, Missile and Space Office, Engineer Research and Development Laboratories, Fort Belvoir, Virginia (4 April 1961).

APPENDIX D

THE LIMIT OF CONVECTION WITH DECREASING PRESSURE

Whatever degree of vacuum is specified for a lunar environmental simulator must be sufficient to eliminate convection as a heat-transfer process. That this may be achieved with vacuums in the neighborhood of 10^{-3} mm Hg will be demonstrated in the following discussion.

The dimensionless ratio known as the Nusselt number, NN , may be expressed (from Ref. 11:315) as:

$$NN_x = 0.378 (NG_x)^{\frac{1}{4}} \quad (8)$$

for a vertical plate in air, where:

0.378 = a coefficient related to the particular gas involved,

subscript x = the vertical distance along the plate at which the heat transfer is being calculated, and

NG = the Grashof number.

Now (from Ref. 11:314):

$$NG_x = \frac{g \beta \theta_{\omega} x^3}{\nu^2} \quad (9)$$

where:

g = the acceleration of gravity,

β = the thermal expansion coefficient,

θ_{ω} = the difference between the temperature of the plate and the temperature outside the boundary layer, and

ν = the kinematic viscosity (dynamic viscosity divided by the density).

Since NN_x is defined as the film heat-transfer coefficient times the reference distance divided by the thermal conductivity of the gas (Ref. 11:314):

$$NN_x = \frac{h_x}{k} \quad (10)$$

we may substitute Eqs. (9) and (10) into Eq. (8) and obtain

$$\frac{h_x}{k} = 0.378 \left(\frac{g \beta \theta_{\omega} x^3}{\nu^2} \right)^{\frac{1}{4}} \quad (11)$$

Solving for h ;

$$h = \frac{0.378 k}{x} \left(\frac{g \beta \theta_w x^3}{\nu^2} \right)^{\frac{1}{4}} \quad (12)$$

Now, k , g , β , θ_w , and x may be considered as constants independent of the gas used in the simulator (Ref. 25:493). Hence, for any gas, the film heat-transfer coefficient may be considered to be inversely proportional to the square root of the kinematic viscosity:

$$h \propto \frac{1}{\nu^{\frac{1}{2}}} \quad (13)$$

If air is chosen as the gas to be used in the simulator, the diminution of h with increasing altitude (decreasing pressure) may be calculated and expressed as a percentage of sea-level free convection. For example, using the NACA standard atmosphere (1947), at

sea level, $h \propto \frac{1}{\sqrt{1.564}} = 0.799$, which is used as the reference value. At 50,000 feet,
 $h \propto \frac{1}{\sqrt{8.175}} = 0.349$, or 43.6 percent of the sea-level reference value.

This process may be continued to 250,000 feet, or 4.09×10^{-2} mm Hg, at which point the tabulated values of ν become increasingly uncertain (even with the more recent model atmospheres). More important, the increase in mean free path of the air molecules must be considered. For a plot of the decrease in convection effectiveness with increasing altitude, see Figure 29.

Table 7 illustrates the increase in mean free path with decreasing pressure (Ref. 24). It is obvious that convection phenomena are meaningless where the mean free path of the molecules is as great as 0.36 inch.

TABLE 7

INCREASE OF MEAN FREE PATH WITH DECREASE IN PRESSURE

Pressure (mm Hg)	Approximate Altitude (feet)	Approximate Mean Free Path (feet)
10^{-2}	230,000	0.00007
10^{-3}	300,000	0.03
10^{-4}	350,000	1
10^{-5}	400,000	13
10^{-6}	650,000	500

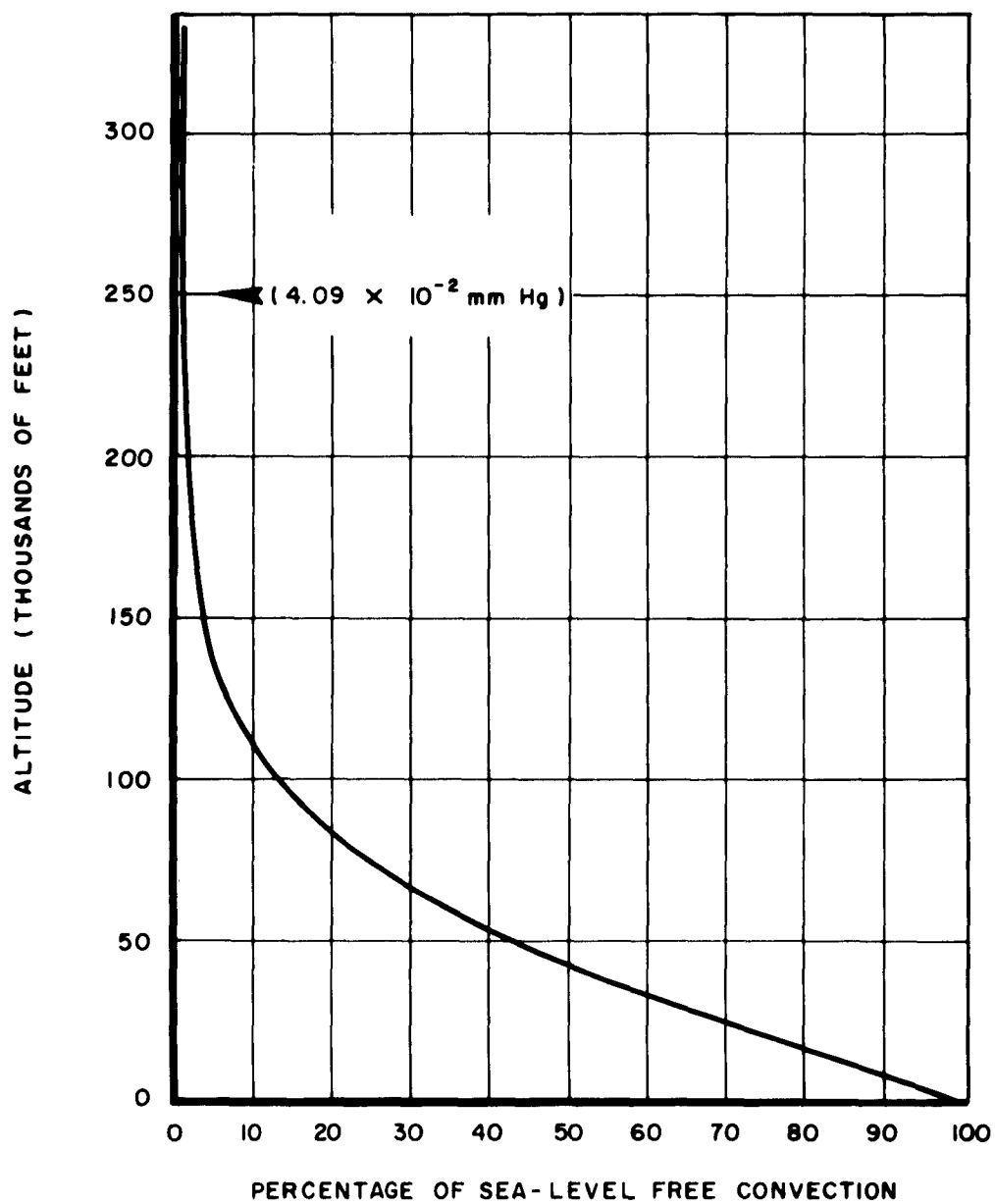


Figure 29. Decrease in Free-Air Convection with Increasing Altitude

APPENDIX E

HIGH-VACUUM FRICTION

The investigation of friction forces under high vacuum dates back to 1939 (Ref. 30:A-4). Unfortunately, all the researchers have apparently investigated the effect of friction under only two conditions: local ambient pressure and "high vacuum." At no time did an investigator make his experiment at various levels of vacuum. Consequently, no one has any idea of where the coefficient of friction starts to increase or where it levels off.*

A leading researcher in the field, Mr. A. Stephenson of Litton Industries, believes that the coefficient of friction may increase up to 10^{-9} mm Hg, at which point there exists the possibility of "cold-welding" due to the removal of the unimolecular film. (Note: This is third-hand information. Mr. Stephenson himself did not mention it in reply to an inquiry on the subject.**)

As an empirical matter, vehicular components subject to high-vacuum friction are tested in vacuums of 9×10^{-7} mm Hg (Ref. 21). If the test item works at 9×10^{-7} mm Hg, it is considered that it will work in cislunar space.*

Perhaps the most comprehensive work on high-vacuum friction has been done by the Advanced Development Laboratory of Litton Systems, Incorporated. This research was sponsored by the Air Force and the results were published in Reference 30.

In this work, the linear motion between two dry, clean, unlubricated surfaces was studied and compared at ambient (about 760 mm Hg) and high-vacuum (10^{-5} to 10^{-6} mm Hg) conditions. A pattern of increased friction was noticed at high vacuum amounting, generally, to twice that at sea level. No attempt was made to determine at what vacuum this took place, although it was understood to be related to the nature of the surface film retained on the specimens.

About the only definite statement that can be made concerning high-vacuum friction is that considerably more work needs to be done. A simple series of tests designed to measure the increase in friction coefficient with increasing vacuum for several materials would be of enormous benefit, not only to those concerned with simulation, but also to designers of space vehicles.

* Letter from Miss L. van der Wal, project engineer, Space Technology Laboratories, Los Angeles, California (21 June 1961).

** Letter from Mr. A. Stephenson, Space Science Laboratory, Litton Systems, Inc., Beverly Hills, California (1 June 1961).

APPENDIX F

HIGH-VACUUM EXPOSURE OF LUNAR ROCK MODELS

During the course of this investigation, several rock samples representative of possible lunar rock were obtained. The general criteria for establishing a rock as a lunar model were much the same as that outlined for dust models. In addition to these criteria, the rocks were selected for their extreme lightness, since it is felt that volcanic processes occurring at one-sixth earth gravity would produce lighter, more vesicular rock than the normal earth specimen (Refs. 16:10, 15:70).

Since the lunar dust is most likely strewn over a rocky rubble or, at best, a rather uneven lava flow, any lunar environmental simulator should have a varying dust layer (in thickness and composition) overlaying a varying rock layer (in thickness and composition). Since porous rock full of bubbles of trapped gases could be dangerous in a lunar simulator chamber, it was decided to test all of the available specimens to see if any of them exploded or cracked under the reduced pressure. Some of the more fragile specimens were also cycled briefly.

The tests were made by "hitch-hiking" a rock sample in a strong container with a built-in leak when a run was made with a dust sample. Figure 16 shows the hitch-hiker container on the wire screen outside the cannister.

None of the rocks did anything more than exfoliate slightly. All of them were sufficiently fragile to chip by handling in any case, so this effect is more apparent than real.

The rocks are shown in Figure 30. They are, from left to right and top to bottom, reticulite from Kilauea volcano (density of 0.03 gm/cc.); basaltic pumice from Kilauea volcano (density of 0.05 to 0.08 gm/cc.); partly decomposed silicic acidic tuff, California; Italian pumice (density of 1.1 g/cc.); basaltic pahoehoe from Kilauea Caldera (density 1.5 to 2.0 gm/cc.); basaltic cinder from Kilauea volcano (density 0.4 to 0.7 gm/cc.); and silicic cinders (red and gray) from near Las Vegas, Nevada.

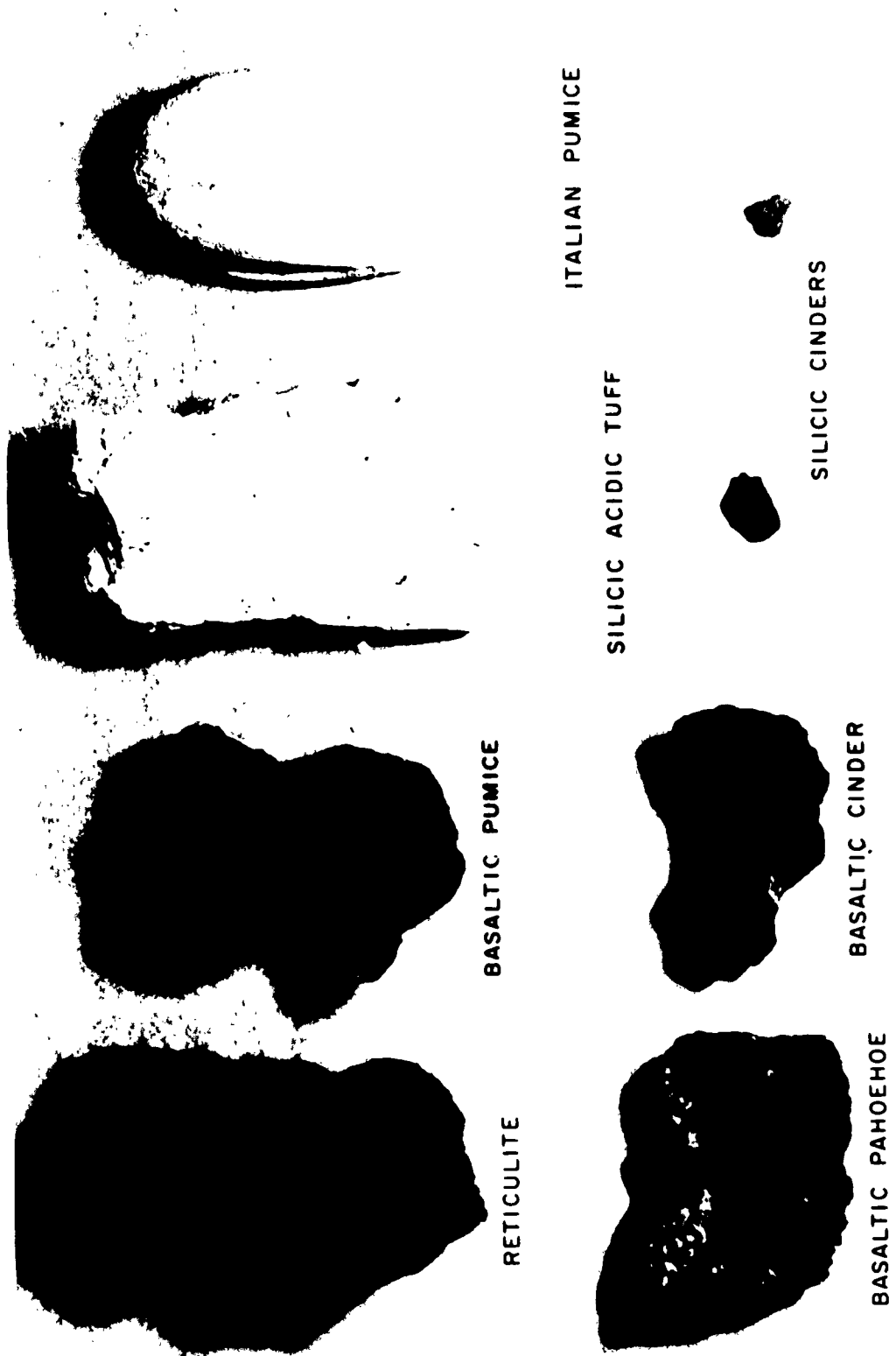


Figure 30. Volcanic Rock Specimens After Exposure to Vacuum

APPENDIX G

A GLOSSARY OF ASTRONOMICAL AND GEOLOGICAL TERMS

<u>accretive</u>	building up a layer of dust or rock by the successive and continuous in-fall of very small amounts of material (In this context, the continuous sweeping out of cosmic dust and debris in the path of the moon.)
<u>acidic</u>	rock high in silica
<u>ash</u>	uncemented volcanic detritus or loose material between 1/4 and 4 mm. in diameter (Technically, the dust specimens tested consisted of both dust and ash.)
<u>basaltic</u>	containing 50 percent plagioclase feldspars and 50 percent ferromagnesian silicates (see silicic)
<u>bombs</u>	a rounded mass of newly congealed magma blown out during a volcanic eruption
<u>caldera</u>	any formation with a volcanic origin and a diameter at least three to four times its depth
<u>cinders</u>	glassy or vesicular lapilli (see lapilli)
<u>cislunar</u>	pertaining to the region of space between the earth and the moon; this part of the solar system
<u>dust</u>	uncemented volcanic detritus less than 1/4 mm. in diameter (Technically, the dust specimens examined consisted of both dust and ash.)
<u>earthshine</u>	the reflected light of the earth on the moon; analogous to moonlight as seen from earth
<u>exfoliation</u>	spontaneous chipping or flaking of a rock
<u>granitic</u>	a silicic rock composed of 50 percent alkali feldspars, 25 percent quartz, and 25 percent plagioclase feldspars and ferromagnesian minerals (see silicic)
<u>lapilli</u>	bombs between 4 and 32 mm. diameter (see bombs)
<u>lunar disk</u>	the image of the moon's surface as seen in a telescope
<u>lunation</u>	a lunar day-night cycle
<u>magma</u>	a naturally occurring silicate melt
<u>maria</u>	the dark areas of the moon, generally thought to be immense lava flows

- pahoehoe rock from a smooth flow of lava
- phreatomagmatic . . pertaining to the contact of a magma with underground waters (A phreatomagmatic eruption is a sort of steam-boiler explosion.)
- pumice light, glassy, vesicular volcanic rock
- reticulite super-light basaltic pumice; also called threadlace scoria
- ring-wall an allusion to the shape and actual relative dimensions of most lunar craters (These craters are very wide in comparison to their depth, so much so that an observer in the middle of one of the big craters could not see the mile or more high "ring-walls." The larger craters are also called "walled-plains" by some writers.)
- rock flour the coarse rock dust produced by a meteoric impact and found in the bottom of the crater
- scoracious slag-like
- selenology the technical term for lunar geology
- silicate a rock containing silicic acid salts
- silicic the rocks typical of continental areas; granites, rhyolite, etc. (These rocks contain large amounts of alkali feldspar, $K(AlSi_3O_8)$, and $Na(AlSi_3O_8)$, and the plagioclase feldspars, $Ca(Al_2Si_2O_8)$.)
- tectonic pertaining to seismic disturbances; probably of minor significance in the production of dust on the moon
- terminator the line dividing the day and night side of the moon
- tuff rock consolidated from volcanic ash
- vesicular full of cavities

LIST OF REFERENCES

1. Aero-Space Laboratories. Selected Lunar Data. Chart. North American Aviation, Inc., Downey, California.
2. Aero-Space Laboratories. Simulated Lunar Dust Experiments. MD 60-287. North American Aviation, Inc., Downey, California. 1 December 1960.
3. Aerospace Division. Space Simulators. Advertising brochure, Tenney Engineering, Inc., Union, New Jersey.
4. Baldwin, R. B. The Face of the Moon. University of Chicago Press, Chicago, Illinois, 1949.
5. Bendix Systems Division. The Bendix Corporation Space Laboratory, Bendix Systems Division. Advertising brochure. Bendix Corporation, Ann Arbor, Michigan.
6. Brandt, J. C. "Density of the Lunar Atmosphere," Science 131: 1606. 27 May 1960.
7. Browne, I. C. and Evans, J. V. "The Moon as a Scatterer of Radio Waves," Radio Astronomy, ed. by Van de Hulst, H. C. (International Astronomical Union Symposium No. 4, August 1955). University Press, Cambridge, UK. 1957.
8. Brunschwig, W., et al. Estimation of the Physical Constants of the Lunar Surface. Ann Arbor, Michigan, 6 June 1961.
9. Crozier, W. D. "Black, Magnetic Spherules in Sediments," Journal of Geophysical Research 65: 2917-2971, September 1960.
10. Derjaguin, B. V. "The Force Between Molecules," Scientific American 203: 47-53. July 1960.
11. Eckert, E. G. and Drake, R. M. Heat and Mass Transfer. McGraw-Hill Book Company, Inc., New York. 1959.
12. Elsmore, B. "Radio Observations of the Lunar Atmosphere." Philosophical Magazine, 2: 1040-6. August 1957.
13. Fielder, G. "The Physical Nature of the Surface of the Moon," Journal of the British Interplanetary Society, 17: 57. March-April 1959.
14. Firsoff, V. A. Our Neighbor Worlds. Philosophical Library, New York. 1953.
15. Firsoff, V. A. Strange World of the Moon. Basic Books, New York. 1959
16. Green, J. "Some Aspects of Lunar Geology." Astronautical Sciences Review 2: 9-16. January-March 1960.
17. Jastrow, R. "The Exploration of the Moon," Scientific American 202: 61-69. May 1960.
18. Kulander, J. Lunar Temperature. AFBMD TR-59-9. Boeing Airplane Company, Seattle, Washington. 30 September 1959.

LIST OF REFERENCES (CONT'D)

19. Land Locomotion Laboratory. "A Soil Value System for Locomotion Mechanics." Research Report No. 5. U. S. Army Land Locomotion Laboratory, Detroit, Michigan. December 1958.
20. Leet, L. D. and Judson, S. Physical Geology. Prentice-Hall, Inc., New York. 1959.
21. LeVantine, A. Space Thermal Environment Simulation Facility. Space Technology Laboratories, Inc., Los Angeles, California. 31 October 1960.
22. Moore, P. A Guide to the Moon. W. W. Norton and Company, Inc., New York. 1953.
23. Norair Engineering Test Summary No. 91529. Northrop Corporation, Hawthorne, California. 25 May 1961.
24. Series of untitled charts based on 1959 ARDC model atmosphere. Northrop Corporation, Hawthorne, California.
25. Pawsey, J. L. and Bracewell, R. N. Radio Astronomy. Clarendon Press, Oxford, U. K., 1955.
26. Piddington, J. H. and Minnett, H. C. "Microwave Thermal Radiation from the Moon." Australian Journal of Scientific Research 2: 63 (1949).
27. Pope, A. Wind Tunnel Testing. John Wiley and Sons, New York. 1954.
28. Sadow, P. T. Characteristics of and Movement on the Lunar Surface. TN-60-14, Wright Air Development Division, Wright-Patterson Air Force Base, Ohio. 30 August 1960.
29. Space Research Laboratories. Research Leading to the Capability of NASA to Provide a National Lunar Laboratory. Litton Industries, Beverly Hills, California.
30. Research Program on High-Vacuum Friction. TM 60-7, Advanced Development Laboratory, Litton Systems, Incorporated, Beverly Hills, California. 28 December 1960.
31. Urey, H. C. "The Origin and Significance of the Moon's Surface." Vistas in Astronomy: 2 ed. by Beer, A. Pergamon Press (1956) 1667-1680. New York.
32. Urey, H. C. The Planets -- Their Origin and Development. Yale University Press, New Haven, Connecticut. 1952.
33. "Volcanoes" Encyclopedia Britannica, Vol. XXIII. William Benton, Publishers, Chicago, Illinois. 1959.

<p>Aeronautical Systems Division, Wright-Patterson Air Force Base, Ohio. Rpt No. ASD TR 61-595. IMPACT STUDIES ON LUNAR DUST MODELS AT VARIOUS VACUUMS. Final report, Jan 62, 76p. incl illus., tables.</p> <p>Unclassified report</p> <p>An analysis of the factors relevant to lunar environmental simulation show that the dynamic behavior of lunar dust models in various vacuums must be studied to establish the degree of vacuum required of a lunar simulator. Various silicic and basaltic rock dusts were selected as lunar dust models and tested under a range of vacuums. Although crater width measurements indicate lunar dust models do not change their resistance to</p> <p>(over)</p>	<p>UNCLASSIFIED</p> <p>1. Space Environmental Conditions</p> <p>2. Lunar Models</p> <p>I. AFSC Project 8119, Task 811918</p> <p>II. R. L. Geer, 1st Lt, USAF</p> <p>III. Aval fr OTS</p> <p>IV. In ASTIA collection</p> <p>UNCLASSIFIED</p>	<p>UNCLASSIFIED</p> <p>1. Space Environmental Conditions</p> <p>2. Lunar Models</p> <p>I. AFSC Project 8119, Task 811918</p> <p>II. R. L. Geer, 1st Lt, USAF</p> <p>III. Aval fr OTS</p> <p>IV. In ASTIA collection</p> <p>UNCLASSIFIED</p>
<p>impact at vacuums beyond 1×10^{-3} mm Hg, depth of penetration measurements do show a continuous change in resistance up to 1×10^{-5} mm Hg, the limit of the test. The behavior of lunar dust particles depend upon both particle size distribution and particle microstructure. The effects of hold times at vacuum, container walls, dust shallowness, and the composition of the residual atmosphere on dust behavior are analyzed. Recommendations are made for follow-up studies.</p>	<p>UNCLASSIFIED</p> <p>UNCLASSIFIED</p> <p>UNCLASSIFIED</p>	<p>UNCLASSIFIED</p> <p>Impact at vacuums beyond 1×10^{-3} mm Hg, depth of penetration measurements do show a continuous change in resistance up to 1×10^{-5} mm Hg, the limit of the test. The behavior of lunar dust particles depend upon both particle size distribution and particle microstructure. The effects of hold times at vacuum, container walls, dust shallowness, and the composition of the residual atmosphere on dust behavior are analyzed. Recommendations are made for follow-up studies.</p> <p>UNCLASSIFIED</p>

<p>Aeronautical Systems Division, Wright-Patterson Air Force Base, Ohio. Rpt No. ASD TR 61-595. IMPACT STUDIES ON LUNAR DUST MODELS AT VARIOUS VACUUMS. Final report, Jan 62, 76p. incl illus., tables.</p> <p>Unclassified report</p> <p>An analysis of the factors relevant to lunar environmental simulation show that the dynamic behavior of lunar dust models in various vacuums must be studied to establish the degree of vacuum required of a lunar simulator. Various silicic and basaltic rock dusts were selected as lunar dust models and tested under a range of vacuums. Although crater width measurements indicate lunar dust models do not change their resistance to</p> <p>(over)</p>	<p>UNCLASSIFIED</p> <p>1. Space Environmental Conditions</p> <p>2. Lunar Models</p> <p>I. AFSC Project 8119, Task 811918</p> <p>II. R. L. Geer, 1st Lt, USAF</p> <p>III. Aval fr OTS</p> <p>IV. In ASTIA collection</p>	<p>UNCLASSIFIED</p> <p>1. Space Environmental Conditions</p> <p>2. Lunar Models</p> <p>I. AFSC Project 8119, Task 811918</p> <p>II. R. L. Geer, 1st Lt, USAF</p> <p>III. Aval fr OTS</p> <p>IV. In ASTIA collection</p>	<p>UNCLASSIFIED</p> <p>1. Space Environmental Conditions</p> <p>2. Lunar Models</p> <p>I. AFSC Project 8119, Task 811918</p> <p>II. R. L. Geer, 1st Lt, USAF</p> <p>III. Aval fr OTS</p> <p>IV. In ASTIA collection</p>	<p>UNCLASSIFIED</p> <p>1. Space Environmental Conditions</p> <p>2. Lunar Models</p> <p>I. AFSC Project 8119, Task 811918</p> <p>II. R. L. Geer, 1st Lt, USAF</p> <p>III. Aval fr OTS</p> <p>IV. In ASTIA collection</p>	<p>UNCLASSIFIED</p> <p>1. Space Environmental Conditions</p> <p>2. Lunar Models</p> <p>I. AFSC Project 8119, Task 811918</p> <p>II. R. L. Geer, 1st Lt, USAF</p> <p>III. Aval fr OTS</p> <p>IV. In ASTIA collection</p>	<p>UNCLASSIFIED</p> <p>Impact at vacuums beyond 1×10^{-3} mm Hg, depth of penetration measurements do show a continuous change in resistance up to 1×10^{-6} mm Hg, the limit of the test. The behavior of lunar dust particles depend upon both particle size distribution and particle microstructure. The effects of hold times at vacuum, container walls, dust shallowness, and the composition of the residual atmosphere on dust behavior are analyzed. Recommendations are made for follow-up studies.</p>	<p>UNCLASSIFIED</p> <p>Impact at vacuums beyond 1×10^{-3} mm Hg, depth of penetration measurements do show a continuous change in resistance up to 1×10^{-6} mm Hg, the limit of the test. The behavior of lunar dust particles depend upon both particle size distribution and particle microstructure. The effects of hold times at vacuum, container walls, dust shallowness, and the composition of the residual atmosphere on dust behavior are analyzed. Recommendations are made for follow-up studies.</p>	<p>UNCLASSIFIED</p> <p>Impact at vacuums beyond 1×10^{-3} mm Hg, depth of penetration measurements do show a continuous change in resistance up to 1×10^{-6} mm Hg, the limit of the test. The behavior of lunar dust particles depend upon both particle size distribution and particle microstructure. The effects of hold times at vacuum, container walls, dust shallowness, and the composition of the residual atmosphere on dust behavior are analyzed. Recommendations are made for follow-up studies.</p>	<p>UNCLASSIFIED</p> <p>1. Space Environmental Conditions</p> <p>2. Lunar Models</p> <p>I. AFSC Project 8119, Task 811918</p> <p>II. R. L. Geer, 1st Lt, USAF</p> <p>III. Aval fr OTS</p> <p>IV. In ASTIA collection</p>	<p>UNCLASSIFIED</p> <p>1. Space Environmental Conditions</p> <p>2. Lunar Models</p> <p>I. AFSC Project 8119, Task 811918</p> <p>II. R. L. Geer, 1st Lt, USAF</p> <p>III. Aval fr OTS</p> <p>IV. In ASTIA collection</p>	<p>UNCLASSIFIED</p> <p>1. Space Environmental Conditions</p> <p>2. Lunar Models</p> <p>I. AFSC Project 8119, Task 811918</p> <p>II. R. L. Geer, 1st Lt, USAF</p> <p>III. Aval fr OTS</p> <p>IV. In ASTIA collection</p>
---	---	---	---	---	---	--	--	--	---	---	---